Journal of Computational Mathematics
Vol.33, No.6, 2015, 642–684.

http://www.global-sci.org/jcm
doi:10.4208/jcm.1509-m4414

# NEW TRIGONOMETRIC BASIS POSSESSING EXPONENTIAL SHAPE PARAMETERS*

Yuanpeng Zhu
*School of Mathematics and Statistics, Central South University, Changsha 410083, China*
*School of Mathematical Sciences, University of Science and Technology of China, Hefei 230026, China*
*Email: zhuyuanpeng@csu.edu.cn*
Xuli Han [1)]
*School of Mathematics and Statistics, Central South University, Changsha 410083, China*
*Email: xlhan@csu.edu.cn*

**Abstract**

Four new trigonometric Bernstein-like basis functions with two exponential shape parameters are constructed, based on which a class of trigonometric Bézier-like curves, analogous to the cubic Bézier curves, is proposed. The corner cutting algorithm for computing the trigonometric Bézier-like curves is given. Any arc of an ellipse or a parabola can be represented exactly by using the trigonometric Bézier-like curves. The corresponding trigonometric Bernstein-like operator is presented and the spectral analysis shows that the trigonometric Bézier-like curves are closer to the given control polygon than the cubic Bézier curves. Based on the new proposed trigonometric Bernstein-like basis, a new class of trigonometric B-spline-like basis functions with two local exponential shape parameters is constructed. The totally positive property of the trigonometric B-spline-like basis is proved. For different values of the shape parameters, the associated trigonometric B-spline-like curves can be $C^2 \cap FC^3$ continuous for a non-uniform knot vector, and $C^3$ or $C^5$ continuous for a uniform knot vector. A new class of trigonometric Bézier-like basis functions over triangular domain is also constructed. A de Casteljau-type algorithm for computing the associated trigonometric Bézier-like patch is developed. The conditions for $G^1$ continuous joining two trigonometric Bézier-like patches over triangular domain are deduced.

*Mathematics subject classification:* 65D07, 65D18.
*Key words:* Trigonometric Bernstein-like basis, Trigonometric B-spline-like basis, Corner cutting algorithm, Totally positive property, Shape parameter, Triangular domain.

## 1. Introduction

Trigonometric splines and polynomials have attracted widespread interest within CAGD (Computer Aided Geometric Design), particularly within curve design, see for example [17,29, 30,37,39,45–47,50] and the references therein. In [18–22], some quadratic and cubic trigonometric polynomial splines with shape parameters were shown. In [25], a class of cubic trigonometric Bézier curves with two shape parameters was proposed, which is an extension of the cubic trigonometric Bézier curves with a shape parameter given in [20]. In [52], a class of C-Bézier curves was constructed in the space $\text{span}\{1, t, \sin t, \cos t\}$, where the length of the interval serves as shape parameter. The C-Bézier curves can exactly represent the ellipse and

* Received July 25, 2013 / Revised version received October 14, 2014 / Accepted September 21, 2015 / Published online November 17, 2015 /
1) Corresponding author

the sine curves. When the length of the interval tends to zero, the C-Bézier curves yield the classical cubic Bézier curves. Geometric interpretation of the change of the shape parameter for C-Bézier curves was given in [26]. In [6], it was pointed out that the critical length for the space $\text{span}\{1, t, \sin t, \cos t\}$ is $2\pi$, which means that Extended Complete Chebyshev (ECC) space for the space $\text{span}\{1, t, \sin t, \cos t\}$ exists only on interval of length less than $2\pi$. In [2], this restriction was overcome by substituting ECC-space with the Canonical Complete Chebyshev (CCC) space.

For modifications of the curve form, it is worth to study the practical methods for adjusting curves by using tension shape parameters. In [10], a kind of variable degree polynomial splines was constructed in the space $\text{span}\{1, t, (1-t)^p, t^q\}$, where $p, q$ are two arbitrary integers greater than or equal to 3 and used as tension shape parameters. In [31,32], this space was proved to be a Quasi Extended Chebyshev (QEC) space and studied by using the blossom approach. Later, in [15], the space $\text{span}\{1, t, t^2, ..., t^{n-2}, (1-t)^p, t^q\}$ was investigated by using a direct approach based on elementary analytic properties of the space, where $p, q \geq n+1$ are any real numbers. Based on the fact that the space $\text{span}\{1, t, t^2, ..., t^{n-2}, (1-t)^p, t^q\}$ is a QEC-space for any real numbers $p, q \geq n-1$ and $\max(p, q) > n-1$, the dimension elevation process for the space was further studied via blossom approach, see [33–36]. Recently, in [3], the totally positivity property of the variable degree polynomial spline basis was proved within the general framework of CCC-space. For the problems of shape preserving interpolation and approximation, the variable degree polynomial splines show great potential applications, see [11,13,14,16]. In [54], a kind of $\alpha\beta$-Bernstein-like basis with two exponential shape parameters was constructed in the space $\text{span}\{1, 3t^2 - 2t^3, (1-t)^\alpha, t^\beta\}$, which forms an optimal normalized totally positive basis and includes the cubic Said-Ball basis and the cubic Bernstein basis as special cases. In [42], by using an iterative integral method, changeable degree spline basis functions were defined. In [44], the explicit representations of changeable degree spline basis functions were given. In [24], five trigonometric blending functions possessing two exponential shape parameters were constructed in the space $\text{span}\{1, \sin t(1-\sin t)^{\alpha-1}, \cos t(1-\cos t)^{\beta-1}, (1-\sin t)^\alpha, (1-\cos t)^\beta\}$, based on which a class of trigonometric B-spline-like curves with three local shape parameters and a global shape parameter were proposed. In [27], these five trigonometric blending functions were further extended to a general case. It was pointed out in [12] that for constructing space curves, $C^2 \cap FC^3$ is a reasonable smoothness property since such continuity can ensure that the motion of a point on the generated curves have a continuous acceleration and that the generated curves possess continuous curvature vectors and torsion. And by using a modification of the $C^4$ quintic splines, a class of $C^2 \cap FC^3$ spline curves possessing tension shape properties was described in [12]. Based on the quartic Bernstein basis functions, a class of general quartic spline curves with three local shape parameters was proposed in [23]. The given spline curves can be $C^2 \cap GC^3$ continuous by fixing some values of the curves' shape parameters.

Since tensor product Bézier patch is the direct extension of Bézier curve, we can get rectangular patches with shape parameters through the above mentioned new curves. However, the Bernstein-Bézier surface over the triangular domain is not a tensor product patch exactly. Therefore, we cannot get triangular surfaces with an adjustable shape through the method of tensor product. During the last years, some researchers have put many efforts on the establishments of new bases over triangular domain with shape parameters, see for example [8,43,48,49,51,53]. In [43], Shen and Wang proposed a kind of Bernstein-like basis with a shape parameter, which was a triangular domain extension of the p-Bézier basis of order 3 given in [39]. In [48], Wei, Shen and Wang extended the C-Bézier basis on the univariate domain given in [52] to a new Bézier-like basis on the triangular domain, which possess a shape parameter and can be used to generate some surfaces whose boundaries are arcs of ellipse. In [53], a kind of triangular Bernstein-Bézier-type patch with three exponential shape parameters was proposed.

The purpose of this paper is to present four new trigonometric Bernstein-like basis functions possessing two exponential shape parameters constructed in the trigonometric function space $\text{span}\{1, \sin^2 t, (1-\sin t)^\alpha, (1-\cos t)^\beta\}$ and a new class of trigonometric Bézier-like basis over triangular domain possessing three exponential shape parameters. The given trigonometric Bernstein-like operator and the associated spectral analysis can help to further understand the corresponding trigonometric Bézier-like curves. The proposed trigonometric B-spline-like curves with two local exponential shape parameters have $C^2 \cap FC^3$ continuity at single knots and can be $C^3$ even $C^5$ continuous for particular choice of the shape parameters. The exponential shape parameters serve as tension shape parameters and have a predictable adjusting role on the corresponding curves and patches.

The rest of this paper is organized as follows. Section 2 gives the construction and properties of the trigonometric Bernstein-like basis functions. The corresponding trigonometric Bézier-like curves and trigonometric Bernstein-like operator are shown. In section 3, trigonometric B-spline-like curves with two local exponential shape parameters are presented. In section 4, a class of trigonometric Bézier-like patch over triangular domain with three exponential shape parameters is presented. And finally, conclusions are given in section 5.

## 2. Trigonometric Bernstein-like Basis Functions

### 2.1. Preliminaries

In this subsection, we shall give the necessary background on Extended Completed Chebyshev (ECC) space and Quasi Extended Chebyshev (QEC) space with special emphasis on weight functions, blossom and Quasi Bernstein-like basis. We will merely mention very few results necessary for a good understanding for the present paper, and more details can be found in [31–36, 40].

Let $I$ denote a given closed bounded interval $[a, b]$, with $a < b$. We call function space $(u_0, u_1, u_2, u_3)$ a 4-dimensional ECC-space in canonical form generated by positive weight functions $w_j \in C^{3-j}(I)$ provided that

$$\begin{aligned} u_0(t) &= w_0(t), \\ u_1(t) &= w_0(t)\int_a^t w_1(t_1)dt_1, \\ u_2(t) &= w_0(t)\int_a^t w_1(t_1)\int_a^{t_1} w_2(t_2)dt_2dt_1, \\ u_3(t) &= w_0(t)\int_a^t w_1(t_1)\int_a^{t_1} w_2(t_2)\int_a^{t_2} w_3(t_3)dt_3dt_2dt_1. \end{aligned}$$

It is well known that 4-dimensional function space $(u_0, u_1, u_2, u_3)$ is an ECC-space on $I$ if and only if for any $k$, $0 \le k \le 3$, any nontrivial linear combination of the elements of the subspace $(u_0, \ldots, u_k)$ has at most $k$ zeros (counting multiplicities). And 4-dimensional function space $(u_0, u_1, u_2, u_3) \subset C^2(I)$ is a QEC-space on $I$ if for any nontrivial linear combination of the elements of the space vanishes at most three times in $I$, counting multiplicities as far as possible for functions in $C^2(I)$, that is, up to three, see [33–36].

A basis $(u_0, u_1, u_2, u_3)$ is said to be totally positive on $[a, b]$ if, for any sequence of points $a \le t_0 < t_1 < \cdots < t_3 \le b$, the collocation matrix $(u_j(t_i))_{0\le i,j\le 3}$ is totally positive, that is, all its minors are nonnegative. For a given function space possessing totally positive basis, the normalized optimal totally positive basis (i.e. the normalized B-basis) is a normalized totally positive basis from which all other totally positive bases can be deduced by multiplication by a (regular) totally positive matrix. Such normalized optimal totally positive basis is unique and has optimal shape preserving properties, see [6], in the sense that the curves they defined best imitate the corresponding control polygon, such as the monotonicity and convexity of the control polygon are inherited by the curves defined by such basis, see [4].

Osculating flats allow a natural generalization of the blossoming principle. Assume the 4-dimensional $\mathcal{E} \subset C^2$ to contain constants and to be 4-dimensional on $I$. Select three functions $\Phi_1, \Phi_2, \Phi_3$ in $\mathcal{E}$ so that $(1, \Phi_1, \Phi_2, \Phi_3)$ forms a basis of $\mathcal{E}$. We set a mother-function $\Phi := (\Phi_1, \Phi_2, \Phi_3) : I \to \mathbb{R}^3$. This function being $C^2$ on $I$, for any nonnegative integer $i \le 2$, we can consider its osculating flat of order $i$ at $x \in I$, defined as the affine space passing through $\Phi(x)$ and the direction of which is spanned by $\Phi'(x), \ldots, \Phi^{(i)}(x)$, i.e.,

$$\mathrm{Osc}_i\Phi(x) := \left\{ \Phi(x) + \lambda_1\Phi'(x) + \ldots + \lambda_i\Phi^{(i)}(x) \,\middle|\, \lambda_1, \ldots, \lambda_i \in \mathbb{R} \right\}.$$

Choose any positive integers $\mu_1, \ldots, \mu_r$, with $\sum_{i=1}^{r} \mu_i = 3$, and any pairwise distinct $a_1, \ldots, a_r$ in $I$. Then, if ever the $r$ osculating flats $\mathrm{Osc}_{3-\mu_i}\phi(a_i)$, $1 \le i \le r$, have a unique common point, we define the blossom of $\Phi$ as the function $\varphi := (\varphi_1, \ldots, \varphi_3) : I^3 \to \mathbb{R}^3$ such that

$$\{\varphi(x_1, x_2, x_3)\} := \bigcap_{i=0}^{r} \mathrm{Osc}_{3-\mu_i}\Phi(a_i), \tag{2.1}$$

for any 3-tuple $(x_1, x_2, x_3)$ which is equal to $(a_1^{[\mu_1]}, \ldots, a_r^{[\mu_r]})$ up to permutation, where

$$(a_1^{[\mu_1]}, \ldots, a_r^{[\mu_r]}) := (\underbrace{a_1, \ldots, a_1}_{\mu_1}, \ldots, \underbrace{a_r, \ldots, a_r}_{\mu_r}).$$

This blossom satisfies three important properties: symmetry, diagonal property and pseudo-affinity, see [33–36]. We want to highlight the fact that blossom exists in space $\mathcal{E} \subset C^2$ is equivalent to that its differential space $D\mathcal{E}$ is an QEC-space on $I$, see Theorem 3.1 in [34].

For any $(a, b) \in I^2$, the four points $\Pi_i(a, b) := \varphi(a^{[n-i]}, b^{[i]})$, $i = 0, 1, 2, 3$ are called the Chebyshev-Bézier points of $\varphi$ with respect to $(a, b)$. When $a = b$, we have $\Pi_i(a, b) = \varphi(a^{[3]})$, for all $i = 0, 1, 2, 3$. When $a \ne b$, the Chebyshev-Bézier points are obtained as

$$\begin{aligned} &\Pi_0(a, b) = \Phi(a), \quad \Pi_3(a, b) = \Phi(b), \\ &\{\Pi_i(a, b)\} = \mathrm{Osc}_i\Phi(a) \cap \mathrm{Osc}_{3-i}\Phi(b), \quad 1 \le i \le 2. \end{aligned} \tag{2.2}$$

In addition, when $a \ne b$, the three properties of the blossom make it possible to develop a de Casteljau type evaluation algorithm starting from the points $\Pi_i(a, b)$. At the $n$th step of this algorithm we can obtain the values of $\varphi$ as affine combinations of the Chebyshev-Bézier points

$$\Phi(x) = \sum_{i=0}^{3} B_i^{(a,b)}(x)\Pi_i(a, b), \quad \sum_{i=0}^{3} B_i^{(a,b)}(x) = 1, \quad x \in I. \tag{2.3}$$

Due to $(1, \Phi_1, \Phi_2, \Phi_3)$ being a basis of $\mathcal{E}$, the affine flat spanned by the image of $\Phi$ is the whole space $\mathbb{R}^3$. It follows from (2.3) that the points $\Pi_0(a,b), \Pi_1(a,b), \Pi_2(a,b)$ and $\Pi_3(a,b)$ are affinely independent. In addition, the so obtained functions $B_i^{(a,b)}$, $i = 0,1,2,3$ form a basis of $\mathcal{E}$ which are called the Quasi Bernstein-like basis with respect to $(a,b)$, see [33–36].

### 2.2. Construction of trigonometric Bernstein-like basis functions

In this subsection, for any real numbers $\alpha, \beta \in [2, +\infty)$, $t \in [0, \pi/2]$, we shall work with the trigonometric space $T_{\alpha,\beta} := \text{span}\left\{1, \sin^2 t, (1-\sin t)^{\alpha}, (1-\cos t)^{\beta}\right\}$. The associated mother-function is defined as follows

$$\Phi(t) := \left(\sin^2 t, (1-\sin t)^{\alpha}, (1-\cos t)^{\beta}\right), \quad t \in [0, \pi/2]. \tag{2.4}$$

In the following theorem, we shall show that the following space

$$DT_{\alpha,\beta} := span\left\{2\sin t\cos t, -\alpha\cos t(1-\sin t)^{\alpha-1}, \beta\sin t(1-\cos t)^{\beta-1}\right\}$$

is a 3-dimensional QEC-space on $t \in [0, \pi/2]$.

**Theorem 2.1.** *For any real numbers $\alpha, \beta \in [2, +\infty)$, the space $DT_{\alpha,\beta}$ is a 3-dimensional QEC-space on $[0, \pi/2]$.*

*Proof.* For any $\xi_i \in \mathbb{R}$, $t \in [0, \pi/2]$, we consider a linear combination

$$\xi_0\left[2\sin t\cos t\right] + \xi_1\left[-\alpha\cos t(1-\sin t)^{\alpha-1}\right] + \xi_2\left[\beta\sin t(1-\cos t)^{\beta-1}\right] = 0. \tag{2.5}$$

For $t = 0$, from (2.5), we can immediately obtain $\xi_1 = 0$. Similarly, for $t = \pi/2$, from (2.5), we have $\xi_2 = 0$. And finally, we have $\xi_0 = 0$. Thus the space $DT_{\alpha,\beta}$ is a 3-dimensional space.

We shall prove the space $DT_{\alpha,\beta}$ is a 3-dimensional QEC-space on $[0, \pi/2]$ by two steps. Firstly, we prove that the space $DT_{\alpha,\beta}$ is a 3-dimensional ECC space in $(0, \pi/2)$. For any $t \in [a,b] \subset (0, \pi/2)$, let

$$\begin{aligned} u(t) &= \left[-\frac{(1-\sin t)^{\alpha-1}}{\sin t}\right]' \\ &= \frac{1}{\sin^2 t}\left[(\alpha-1)\sin t\cos t(1-\sin t)^{\alpha-2} + \cos t(1-\sin t)^{\alpha-1}\right], \end{aligned}$$

and

$$\begin{aligned} v(t) &= \left[\frac{(1-\cos t)^{\beta-1}}{\cos t}\right]' \\ &= \frac{1}{\cos^2 t}\left[(\beta-1)\sin t\cos t(1-\cos t)^{\beta-2} + \sin t(1-\cos t)^{\beta-1}\right]. \end{aligned}$$

By directly computing, we get

$$\begin{aligned} u'(t) = \frac{-1}{\sin^3 t} \Big\{ &\sin^2 t \Big[ (1-\sin t)^{\alpha-1} + (\alpha-1)\sin t(1-\sin t)^{\alpha-2} \\ &+(\alpha-1)(\alpha-2)\cos^2 t(1-\sin t)^{\alpha-3} \Big] + 2\cos^2 t \Big[ (1-\sin t)^{\alpha-1} \\ &+(\alpha-1)\sin t(1-\sin t)^{\alpha-2} \Big] \Big\} < 0, \\ v'(t) = \frac{1}{\cos^3 t} \Big\{ &\cos^2 t \Big[ (1-\cos t)^{\beta-1} + (\beta-1)\cos t(1-\cos t)^{\beta-2} \\ &+(\beta-1)(\beta-2)\sin^2 t(1-\cos t)^{\beta-3} \Big] + 2\sin^2 t \Big[ (1-\cos t)^{\beta-1} \\ &+(\beta-1)\cos t(1-\cos t)^{\beta-2} \Big] \Big\} > 0. \end{aligned}$$

Thus for the Wronskian of $u(t)$ and $v(t)$, we have

$$W(u,v)(t) = u(t)v'(t) - u'(t)v(t) > 0, \quad \forall t \in [a,b].$$

For $t \in [a,b]$, we define the following weight functions

$$\begin{aligned} w_0(t) &= 2\sin t \cos t, \\ w_1(t) &= Au(t) + Bv(t), \\ w_2(t) &= C\frac{W(u,v)(t)}{[Au(t)+Bv(t)]^2}, \end{aligned}$$

where $A, B, C$ are three arbitrary positive real numbers. Obviously, these weight functions $w_i(t)$ $(i = 0,1,2)$ are bounded, positive and $C^\infty$ on $[a,b]$. Consider the following ECC-space defined by the weight functions $w_i(t)$ $(i = 0,1,2)$

$$\begin{aligned} u_0(t) &= w_0(t), \\ u_1(t) &= w_0(t)\int_a^t w_1(t_1)dt_1, \\ u_2(t) &= w_0(t)\int_a^t w_1(t_1)\int_a^{t_1} w_2(t_2)dt_2 dt_1, \end{aligned}$$

after some simple computation, we can see that these functions $u_i(t)$, $i = 0,1,2$ are in fact some linear combinations of the three functions $2\sin t\cos t$, $-\alpha\cos t(1-\sin t)^{\alpha-1}$, $\beta\sin t(1-\cos t)^{\beta-1}$, which indicates that the space $DT_{\alpha,\beta}$ is a ECC-space on $[a,b]$. Since $[a,b]$ are arbitrary subinterval of $(0,\pi/2)$, we can conclude that the space $DT_{\alpha,\beta}$ is an ECC-space in $(0,\pi/2)$.

Secondly, we further prove that the space $DT_{\alpha,\beta}$ is also a QEC-space on $[0,\pi/2]$. For this purpose, we need to prove that any nonzero element of the space $DT_{\alpha,\beta}$ has at most 2 zeroes on $[0,\pi/2]$ (counting multiplicities as far as possible up to 2). Consider any nonzero function

$$G(t) = C_0\left[2\sin t\cos t\right] + C_1\left[-\alpha\cos t(1-\sin t)^{\alpha-1}\right] + C_2\left[\beta\sin t(1-\cos t)^{\beta-1}\right],$$

where $t \in [0,\pi/2]$. Since the space $DT_{\alpha,\beta}$ is an ECC-space in $(0,\pi/2)$, $G(t)$ has at most two zeroes in $(0,\pi/2)$. Let us assume that the function $G(t)$ vanishes at 0, then we have $C_1 = 0$. In this case, if $C_2 = 0$, then $G(t)$ has a singular zero at 0 and a singular zero at $\pi/2$. If $C_0 = 0$, it can be easily checked that 0 is a double zero of $G(t)$ (counting multiplicities as far as possible up to 2). If $C_0C_2 > 0$, $G(t)$ vanishes exactly one time at 0 and it does not vanish anywhere on $(0, \pi/2]$. If $C_0C_2 < 0$, $G(t)$ vanishes exactly one time at 0 and it does not vanish at $\pi/2$. Moreover, for the following function

$$K(t) := 2C_0 \cos t + C_2\beta(1 - \cos t)^{\beta-1}, \quad t \in \left[0, \frac{\pi}{2}\right],$$

direct computation gives that

$$K'(t) = -2C_0 \sin t + C_2\beta(\beta - 1) \sin t(1 - \cos t)^{\beta-2},$$

it follows that $K(t)$ is a monotonic function on $[0, \pi/2]$. From these together with $K(0)K(\pi/2) = 2\beta C_0C_2 < 0$, we can see that $K(t)$ has exactly one zero in $(0, \pi/2)$, thus we can immediately conclude that $G(t) = \sin tK(t)$ (notice that $C_1 = 0$ for the current case) has exactly one zero in $(0, \pi/2)$. Similarly, for the case that $G(t)$ vanishes at $\pi/2$, we can also deduce that the function $G(t)$ has at most 2 zeroes on $[0, \pi/2]$ (counting multiplicities as far as possible up to 2). Summarizing, the space $DT_{\alpha,\beta}$ is a QEC-space on $[0, \pi/2]$. □

Since the space $DT_{\alpha,\beta}$ is a QEC-space on $[0, \pi/2]$, by Theorem 3.1 of [34] we can see that blossom exists in $T_{\alpha,\beta}$, which implies that the new space $T_{\alpha,\beta}$ is suited for curve design. By Theorem 2.18 of [34], we can also know that the space $T_{\alpha,\beta}$ has a normalized Quasi Bernstein-like basis on $[0, \pi/2]$. In the following theorem, we shall give the Chebyshev-Bézier points of the mother-function $\Phi(t)$ defined in (2.4) and give the associated trigonometric Bernstein-like basis $T_i := T_i^{(0,\pi/2)}$ of the space $T_{\alpha,\beta}$.

**Theorem 2.2.** *For any $\alpha, \beta \in [2, +\infty)$, the four Chebyshev-Bézier points $\Pi_i := \Pi_i(0, \pi/2)$ of the mother-function $\Phi(t)$ defined in (2.4) are given by*

$$\Pi_0 = (0, 1, 0), \quad \Pi_1 = (0, 0, 0), \quad \Pi_2 = (1, 0, 0), \quad \Pi_3 = (1, 0, 1). \tag{2.6}$$

*The four associated trigonometric Bernstein-like basis functions of the space $T_{\alpha,\beta}$ are given by*

$$\begin{cases} T_0(t) = (1 - \sin t)^{\alpha}, \\ T_1(t) = 1 - \sin^2 t - (1 - \sin t)^{\alpha}, \\ T_2(t) = 1 - \cos^2 t - (1 - \cos t)^{\beta}, \\ T_3(t) = (1 - \cos t)^{\beta}. \end{cases} \tag{2.7}$$

*And the system of functions $(T_0(t), T_1(t), T_2(t), T_3(t))$ forms an optimal normalized totally positive basis of the space $T_{\alpha,\beta}$.*

*Proof.* For any $\alpha, \beta \in [2, +\infty)$, from the definition of the mother-function $\Phi(t)$, we have

$$\Phi(0) = (0, 1, 0), \qquad \Phi\left(\frac{\pi}{2}\right) = (1, 0, 1),$$

$$\Phi'(0) = (0, -\alpha, 0), \qquad \Phi'\left(\frac{\pi}{2}\right) = (0, 0, \beta),$$

$$\Phi''(0) = (2, \alpha^2 - \alpha, 0), \qquad \Phi''\left(\frac{\pi}{2}\right) = (-2, 0, \beta^2 - \beta).$$

Thus, by simply computing, we get

$$\Pi_0 = \Phi(0) = (0,1,0), \qquad \Pi_3 = \Phi(1) = (1,0,1),$$
$$\{\Pi_1\} = \mathrm{Osc}_1\Phi(0) \cap \mathrm{Osc}_2\Phi(1) = (0,0,0), \qquad \{\Pi_2\} = \mathrm{Osc}_2\Phi(0) \cap \mathrm{Osc}_1\Phi(1) = (1,0,0).$$

For any $t \in [0, \pi/2]$, from $\Phi(t) = \sum_{i=0}^{3} T_i(t)\Pi_i$, we have

$$\begin{cases} T_2(t) + T_3(t) = \sin^2 t, \\ T_0(t) = (1-\sin t)^{\alpha}, \\ T_3(t) = (1-\cos t)^{\beta}. \end{cases} \tag{2.8}$$

Thus from (2.8) together with $\sum_{i=0}^{3} T_i(t) = 1$, we can easily deduce the expressions of the basis functions $T_i(t)$, $i = 0,1,2,3$.

It can be easily checked that the new basis has the following important end-point property:

- $T_0(0) = 1$, and $T_0(t)$ vanishes 3 times at $\pi/2$ (counting multiplicities as far as possible up to 3);
- $T_3(\pi/2) = 1$, and $T_3(t)$ vanishes 3 times at 0 (counting multiplicities as far as possible up to 3);
- For $i = 1,2$, $T_i(t)$ vanishes exactly $i$ times at 0 and exactly $(3-i)$ times at $\pi/2$.

For any $\alpha, \beta \in [2, +\infty)$, $t \in [0, \pi/2]$, it is obvious that $T_i(t) \geq 0$ $(i = 0,3)$. And for $T_1(t)$, $T_2(t)$, we have

$$T_1(t) = 1 - \sin^2 t - (1-\sin t)^{\alpha} \geq 1 - \sin^2 t - (1-\sin t)^2 = 2\sin t(1-\sin t) \geq 0,$$
$$T_2(t) = 1 - \cos^2 t - (1-\cos t)^{\beta} \geq 1 - \cos^2 t - (1-\cos t)^2 = 2\cos t(1-\cos t) \geq 0.$$

In addition, $T_i(t)$ $(i = 0,1,2,3)$ is positive strictly in $(0, \pi/2)$. Thus, by Definition 2.10 of [34], we can know that the normalized trigonometric Bernstein-like basis (2.7) is precisely the Quasi Bernstein-like basis of the space $T_{\alpha,\beta}$. And by Theorem 2.18 of [34], we can conclude that the normalized trigonometric Bernstein-like basis (2.7) is exactly the optimal normalized totally positive basis of the space $T_{\alpha,\beta}$ restricted to $[0, \pi/2]$.

For convenience, in the following discussion we will also denote the four trigonometric Bernstein-like basis functions as $T_i(t;\alpha,\beta)$, $i = 0,1,2,3$, or $T_i(t;\alpha)$, $i = 0,1$, $T_i(t;\beta)$, $i = 2,3$. Fig. 2.1 shows some plots of trigonometric Bernstein-like basis functions for some values of the shape parameters.

### 2.3. Construction of the trigonometric Bézier-like curves

**Definition 2.1.** *Given control points $P_i$ $(i = 0,1,2,3)$ in $\mathbb{R}^2$ or $\mathbb{R}^3$. Then*

$$T(t;\alpha,\beta) = \sum_{i=0}^{3} T_i(t;\alpha,\beta)P_i, \quad t \in [0, \pi/2], \alpha, \beta \in [2, +\infty) \tag{2.9}$$

*is called a trigonometric Bézier-like (TB-like for short) curve with two exponential shape parameters $\alpha$ and $\beta$.*

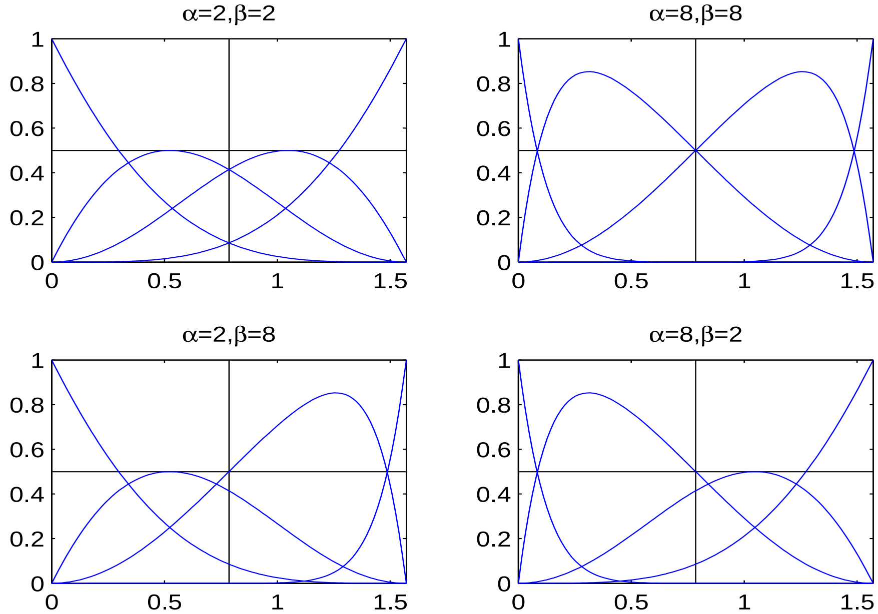


Fig. 2.1. Some plots of trigonometric Bernstein-like basis functions.

Since the trigonometric Bernstein-like basis functions given in (2.7) have the properties of partition of unity, nonnegativity and total positivity, the corresponding TB-like curves given in (2.9) have the properties of affine invariance, convex hull and variation diminishing, which are crucial in curve design. For any $\alpha, \beta \in [2, +\infty)$, direct computation gives the following end-point property of the TB-like curve

$$\begin{cases} T(0;\alpha,\beta) = P_0, & T(\pi/2;\alpha,\beta) = P_3, \\ T'(0;\alpha,\beta) = \alpha(P_1 - P_0), & T'(\pi/2;\alpha,\beta) = \beta(P_3 - P_2). \\ T''(0;\alpha,\beta) = (\alpha^2 - \alpha)(P_0 - P_1) + 2(P_2 - P_1), \\ T''(\pi/2;\alpha,\beta) = (\beta^2 - \beta)(P_3 - P_2) + 2(P_1 - P_2), \\ T'''(0;\alpha,\beta) = (\alpha^3 - 3\alpha^2 + \alpha)(P_1 - P_0), \\ T'''(\pi/2;\alpha,\beta) = (\beta^3 - 3\beta^2 + \beta)(P_3 - P_2). \end{cases} \tag{2.10}$$

We want to point out a fact that for any $\alpha, \beta \in (2, 3)$, $T'''(t;\alpha,\beta)$ cannot be defined in the extremes 0 and $\pi/2$. However, in any case $T'''(0;\alpha,\beta)$ and $T'''(\pi/2;\alpha,\beta)$ can be defined as limits and take those values. We want to highlight that in the following discussion, the values of function will be always defined as limits whenever there is necessary.

The above end-point property implies that for any $\alpha, \beta \in [2, +\infty)$, the TB-like curve has end-point interpolation property and $P_0P_1$, $P_2P_3$ are the tangent lines of the curve at the point $P_0$, $P_3$, respectively. From these, we can see that the TB-like curve has some properties analogous to that of the classical cubic Bézier curve.

### 2.4. Shape control and corner cutting algorithm

For $t \in [0, \pi/2]$, we rewrite the expression of the TB-like curve (2.9) as follows

$$T(t;\alpha,\beta) = P_1 \cos^2 t + P_2 \sin^2 t + T_0(t;\alpha)(P_0 - P_1) + T_3(t;\beta)(P_3 - P_2). \tag{2.11}$$

It is obvious that $T_0(t;\alpha)$ decreases with the increase of $\alpha$ for any fixed $t \in (0, \pi/2)$, which indicates that the generated curves move in the same direction of the edge $P_0 - P_1$ as $\alpha$ increases. On the contrary, as $\alpha$ decreases, the generated curve moves in the opposite direction to the edge $P_0 - P_1$. The shape parameter $\beta$ has the similar effects on the edge $P_3 - P_2$. When $\alpha$ or $\beta$ increases respectively, the curve tends to the point $P_1$ or $P_2$, respectively. And when the shape parameters satisfy $\alpha = \beta$, the curve moves in the same direction or the opposite direction to the edge $P_2 - P_1$ when $\alpha$ increases or decreases, respectively. Thus we can see that the shape parameters $\alpha$ and $\beta$ serve as local tension parameters. Fig. 2.2 shows the TB-like curves with different shape parameters.

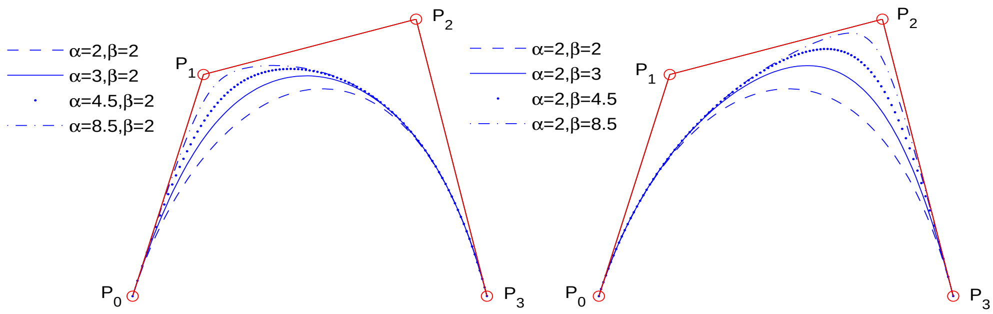


Fig. 2.2. The effect of the shape parameters on the TB-like curves.

Corner cutting algorithm is an efficient and stable process for computing the proposed TB-like curves and it is formed by convex combinations. In order to develop such an algorithm, we rewrite the TB-like curve (2.9) as the following matrix form

$$T(t;\alpha,\beta) = \begin{pmatrix} 1-\sin^2 t & 1-\cos^2 t \end{pmatrix} \times \begin{pmatrix} 1-\sin t & \sin t & 0 \\ 0 & 1-\cos t & \cos t \end{pmatrix}$$

$$\times \begin{pmatrix} \frac{(1-\sin t)^{\alpha-2}}{1+\sin t} & \frac{1+\sin t-(1-\sin t)^{\alpha-2}}{1+\sin t} & 0 & 0 \\ 0 & \frac{\cos t}{\sin t+\cos t} & \frac{\sin t}{\sin t+\cos t} & 0 \\ 0 & 0 & \frac{1+\cos t-(1-\cos t)^{\beta-2}}{1+\cos t} & \frac{(1-\cos t)^{\beta-2}}{1+\cos t} \end{pmatrix} \times \begin{pmatrix} P_0 \\ P_1 \\ P_2 \\ P_3 \end{pmatrix},$$

from these, we can immediately obtain a corner cutting algorithm for computing the TB-like curves. Fig. 2.3 gives an illustration of this algorithm.

### 2.5. The representation of elliptic and parabolic arcs

For $\alpha = \beta = 2$, if the control points are $P_0 = (x_0 + a, y_0)$, $P_1 = (x_0 + a, y_0 + b/2)$, $P_2 = (x_0 + a/2, y_0 + b)$, and $P_3 = (x_0, y_0 + b)$, then the coordinates of the generated curve

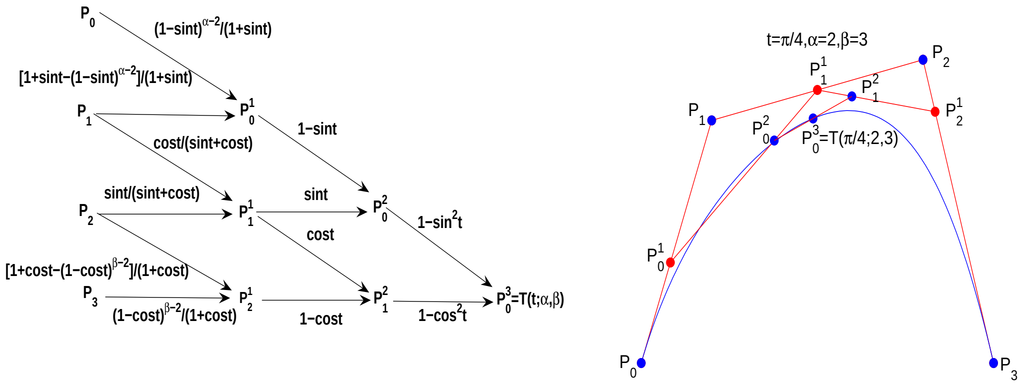


Fig. 2.3. Corner cutting algorithm.

$T(t;2,2)$ are

$$\begin{cases} x(t) = x_0 + a\cos t, \\ y(t) = y_0 + b\sin t, \end{cases} \qquad t \in [0, \pi/2].$$

This expression shows that $T(t;2,2)$ is a quarter of elliptic arc whose center locates at $(x_0, y_0)$. By constraining the parameter $t$ on the desired interval $[\theta_1, \theta_2]$, we can obtain an arc of an ellipse whose starting angle and ending angle are $\theta_1$ and $\theta_2$ respectively.

Furthermore, for $\alpha = \beta = 2, b - a > 0$, if the control points $P_0$, $P_1$, $P_2$ and $P_3$ with respective coordinates $(b, c_2b^2 + c_1b + c_0)$, $(b, c_2b^2 + c_1b + c_0)$, $((b+a)/2, c_2ab + c_1(b+a)/2 + c_0)$, and $(a, c_2a^2 + c_1a + c_0)$, then from (2.9) we obtain

$$\begin{cases} x(t) = (b-a)\cos t + a, \\ y(t) = c_2[(b-a)\cos t + a]^2 + c_1\left[(b-a)\cos t + a\right] + c_0, \end{cases} \qquad t \in [0, \pi/2],$$

which gives a segment of the parabola $y = c_2x^2 + c_1x + c_0$, $x \in [a, b]$.

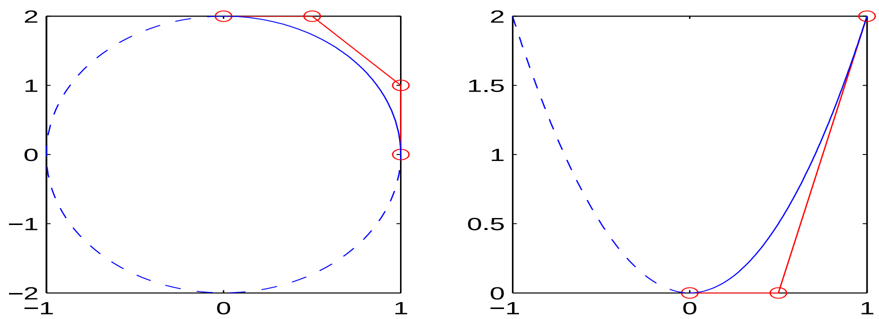

Fig. 2.4. The representation of elliptic and parabolic arcs.

From the above discussion, we can see that any arc of an ellipse or parabola can be represented exactly by using the proposed TB-like curves. Fig. 2.4 shows the elliptic and parabolic segments generated by using the TB-like curves (marked with solid blue lines).

### 2.6. Trigonometric Bernstein-like operator and spectral analysis

Bernstein-like operators are useful to measure the approximation properties of a vector function space and the third greatest eigenvalue of the operators gives a rough idea of the approximation power of the space. The distance of the third greatest eigenvalue to one gives a measure of how close is the curve to its control polygon, see [7]. In this subsection, for any $\alpha = \beta \in [2, +\infty)$, we shall construct a kind of trigonometric Bernstein-like operator by using the trigonometric Bernstein-like basis given in (2.7) and analyze the spectral properties of the operator, which will give a rough estimation about the distance between the TB-like curve $T(t; \alpha, \alpha)$ and the corresponding control polygon.

For $\alpha \in [2, +\infty), t \in [0, \pi/2]$, let

$$f_1(t; \alpha) = \frac{1}{\alpha} T_1(t; \alpha) + \left(1 - \frac{1}{\alpha}\right) T_2(t; \alpha) + T_3(t; \alpha), \tag{2.12}$$

where $T_j(t; \alpha)$, $j = 1, 2, 3$ are the trigonometric Bernstein-like basis functions given in (2.7).

Direct computation gives that

$$\frac{\partial f_1(t; \alpha)}{\partial t} = 2\left(1 - \frac{2}{\alpha}\right) \sin t \cos t + \cos t (1 - \sin t)^{\alpha - 1} + \sin t (1 - \cos t)^{\alpha - 1} > 0,$$

which implies that the function $f_1(t)$ is a strictly increasing function with respect to the variable $t$ for any fixed $\alpha \in [2, +\infty)$. Moveover, it is easy to check that $f_1(t) + f_1(\pi/2 - t) = 1$. From these, we can see that the function $f_1(t; \alpha)$ has some properties analogous to that of the identity function $I(t) = t$.

It is well known that the classical Bernstein operator reproduces the constant function $f_0(t) = 1$ and the identity function $I(t) = t$. We mimic this feature by requiring that the constructed trigonometric Bernstein-like operator reproduces the constant function $f_0(t) = 1$ and the function $f_1(t; \alpha)$ given by (2.12). From [1], we also call $(f_0, f_1)$ a Haar pair.

Since $f_1(t; \alpha)$ is a strictly increasing function with respect to the variable $t$, and $f_1(0; \alpha) = 0$, $f_1(\pi/4; \alpha) = 1/2$, we can see that for any fixed $1/\alpha \in (0, 1/2]$, there exists a unique $t^*_\alpha \in (0, \pi/4]$ such that $f_1(t^*_\alpha; \alpha) = 1/\alpha$. With these preparations, we now can give the definition of the trigonometric Bernstein-like operator $\mathcal{B} : C[0, \pi/2] \to T_{\alpha,\alpha}$ as follows

$$\mathcal{B}(f) = f(0) T_0(t; \alpha) + f(t^*_\alpha) T_1(t; \alpha) + f(\pi/2 - t^*_\alpha) T_2(t; \alpha) + f(\pi/2) T_3(t; \alpha), \tag{2.13}$$

where $f \in C[0, \pi/2]$.

Next, we shall give the spectral analysis on the trigonometric Bernstein-like operator $\mathcal{B}$. Obviously, we have

$$\mathcal{B}(f_0) = f_0(t), \quad \mathcal{B}(f_1) = f_1(t; \alpha),$$

which means that $f_0(t)$ and $f_1(t; \alpha)$ are eigenfunctions corresponding to the eigenvalue $\lambda_0 = \lambda_1 = 1$.

For $\alpha \in [2, +\infty), t \in [0, \pi/2]$, the function

$$f_2(t; \alpha) = 1 - T_0(t; \alpha) - T_3(t; \alpha) \tag{2.14}$$

satisfies $f_2(0;\alpha) = f_2(\pi/2;\alpha) = 0$ and $f_2(t;\alpha) = f_2(\pi/2 - t;\alpha)$, thus we have

$$\begin{aligned}\mathcal{B}(f_2) &= f_2(t^*_\alpha;\alpha)T_1(t;\alpha) + f_2(\pi/2 - t^*_\alpha;\alpha)T_2(t;\alpha)\\ &= f_2(t^*_\alpha;\alpha)\left[T_1(t;\alpha) + T_2(t;\alpha)\right]\\ &= f_2(t^*_\alpha;\alpha)f_2(t;\alpha),\end{aligned}$$

which implies that $f_2(t;\alpha)$ is an eigenfunction corresponding to the eigenvalue $\lambda_{2,\alpha} = f_2(t^*_\alpha;\alpha)$.

In addition, for $\alpha \in [2, +\infty), t \in [0, \pi/2]$, the function

$$f_3(t;\alpha) = T_1(t;\alpha) - T_2(t;\alpha) \tag{2.15}$$

satisfies $f_3(0;\alpha) = f_3(\pi/2;\alpha) = 0$ and $f_3(t;\alpha) = -f_3(\pi/2 - t;\alpha)$, thus we have

$$\begin{aligned}\mathcal{B}(f_3) &= f_3(t^*_\alpha;\alpha)T_1(t;\alpha) + f_3(\pi/2 - t_\alpha;\alpha)T_2(t;\alpha)\\ &= f_3(t^*_\alpha;\alpha)\left[T_1(t;\alpha) - T_2(t;\alpha)\right]\\ &= f_3(t^*_\alpha;\alpha)f_3(t;\alpha),\end{aligned}$$

which implies that $f_3(t;\alpha)$ is an eigenfunction corresponding to the eigenvalue $\lambda_{3,\alpha} = f_3\left(t^*_\alpha;\alpha\right)$.

We shall further show that $0 \le \lambda_{3,\alpha} < \lambda_{2,\alpha} < \lambda_1 = \lambda_0 = 1$. Firstly, it is apparent that $\lambda_{2,\alpha} = f_2\left(t^*_\alpha;\alpha\right) < 1$. Secondly, since $t^*_\alpha \in (0, \pi/4]$, direct computation gives that

$$\begin{aligned}\lambda_{2,\alpha} - \lambda_{3,\alpha} &= f_2(t^*_\alpha;\alpha) - f_3(t^*_\alpha;\alpha)\\ &= 1 - T_0(t^*_\alpha;\alpha) - T_3(t^*_\alpha;\alpha) - T_1(t^*_\alpha;\alpha) + T_2(t^*_\alpha;\alpha)\\ &= 2T_2(t^*_\alpha;\alpha) > 0.\end{aligned}$$

And lastly, for $\alpha \in [2, +\infty)$, from Theorem 2.2, since the system of functions $(T_0(t;\alpha), T_1(t;\alpha), T_2(t;\alpha), T_3(t;\alpha))$ forms a totally positive basis of the space $\mathcal{T}_{\alpha,\alpha}$, for any $0 \le t_0 < t_1 < t_2 < t_3 \le \pi/2$, all the minor determinants of the collocation matrix $(T_j(t_i;\alpha))_{0\le i,j\le 3}$ are nonnegative. Thus, for $t^*_\alpha \in (0, \pi/4]$, we have

$$\begin{vmatrix} T_1\left(t^*_\alpha;\alpha\right) & T_2\left(t^*_\alpha;\alpha\right)\\ T_1\left(\frac{\pi}{4};\alpha\right) & T_2\left(\frac{\pi}{4};\alpha\right)\end{vmatrix} = \left[\frac{1}{2} - \left(1 - \frac{\sqrt{2}}{2}\right)^\alpha\right]\lambda_{3,\alpha} \ge 0,$$

which indicates that $\lambda_{3,\alpha} \ge 0$. This completes the spectral analysis of the proposed trigonometric Bernstein-like operator $\mathcal{B}$ given in (2.13).

From the above discussion, we can see that $\lambda_{2,\alpha}$ is the third greatest eigenvalue of the trigonometric Bernstein-like operator $\mathcal{B}$, and thus $\lambda_{2,\alpha}$ gives a measure of how close is the generated TB-like curve $T(t;\alpha,\alpha)$ to its control polygon. For $\alpha = 2$, it can be checked that $t^*_2 = \pi/4$ and $\lambda_{2,2} = 1 - 2(1 - \sqrt{2}/2)^2 \approx 0.8284$. From [9], we can see that the third greatest eigenvalue of the classical cubic Bernstein operator is $\lambda_2 = 2/3 \approx 0.6667$. These imply that for $\alpha = 2$, the corresponding TB-like curve $T(t;2,2)$ is closer to the given control polygon than the cubic Bézier curve. In general, however, the calculation of the eigenvalue $\lambda_{2,\alpha}$ involves solving a non-linear equation, thus it is quite hard to give the exact solution. Nevertheless, we have

$$\lim_{\alpha\to+\infty} \lambda_{2,\alpha} = 1.$$

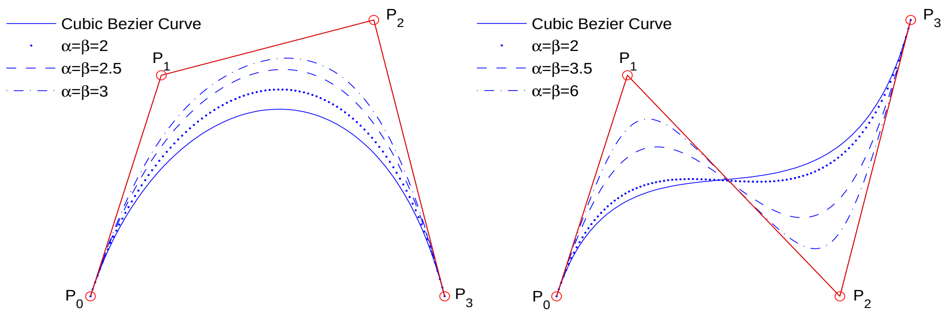


Fig. 2.5. TB-like curves and cubic Bézier curves.

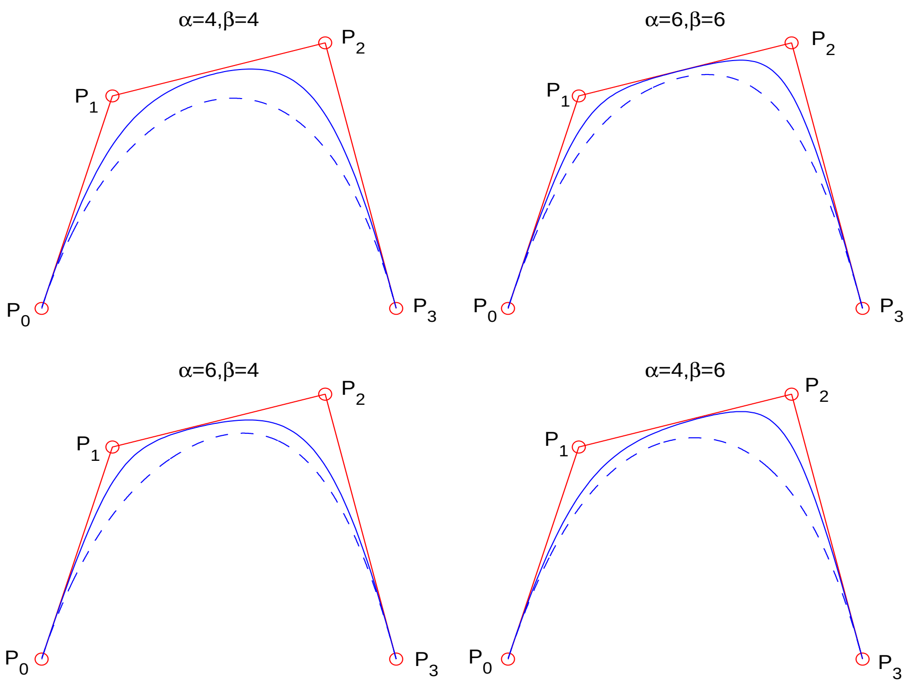


Fig. 2.6. TB-like curves and variable degree polynomial Bézier curves.

Fig. 2.5 shows the comparison between the TB-like curves and the classical cubic Bézier curves under the same control points. It can be seen that as $\alpha = \beta$ increases at the same time, the TB-like curves will be totally closer to the control polygon than the cubic Bézier curves. These imply that the TB-like curves can better maintain the characteristic of the control polygon than the cubic Bézier curves.

Fig. 2.6 shows the comparison between the TB-like curves and the variable degree polynomial Bézier curves given in [10] under the same control points. Clearly, for the same degree, the TB-like curves (solid lines) are closer to the control polygon than the variable degree polynomial Bézier curves (dashed lines).

**Remark 2.1.** For $\alpha = n \geq 2, \beta = m \geq 2, n, m \in \mathbb{Z}^+$, we give a conversion of the proposed

TB-like curve $T(t;n,m)$ to a rational Bézier curve of degree $\max\{2n,2m\}$.

By using the transformation

$$\sin t = 2x/(1+x^2), \quad \cos t = (1-x^2)/(1+x^2), \quad x = \tan(t/2), \quad t \in [0,\pi/2],$$

we can rewrite the four trigonometric Bernstein-like basis functions $T_i(t;n,m)$, $i = 0,1,2,3$ given in (2.7) into the following rational form

$$\begin{cases} T_0(t;n) = \frac{(1-x)^{2n}}{(1+x^2)^n}, \\ T_1(t;n) = \frac{(1-x^2)^2(1+x^2)^{n-2}-(1-x)^{2n}}{(1+x^2)^n}, \\ T_2(t;m) = \frac{4x^2(1+x^2)^{m-2}-2^m x^{2m}}{(1+x^2)^m}, \\ T_3(t;m) = \frac{2^m x^{2m}}{(1+x^2)^m}, \end{cases} \tag{2.16}$$

where $x = \tan(t/2) \in [0,1]$.

After some manipulations, we have

$$(1+x^2)^n = X_{2n}L_{2n}, \quad (1-x)^{2n} = X_{2n}L_{2n}^{(0)},$$

$$(1-x^2)^2(1+x^2)^{n-2} - (1-x)^{2n} = X_{2n}L_{2n}^{(1)},$$

$$4x^2(1+x^2)^{m-2} - 2^m x^{2m} = X_{2m}L_{2m}^{(2)},$$

$$2^m x^{2m} = X_{2m}L_{2m}^{(3)},$$

where $X_{2n} = (1,x,\ldots,x^{2n})$, $L_{2n} = (l_0,l_1,\ldots,l_{2n})^T$, $L_{2n}^0 = (l_0^{(0)},l_1^{(0)},\ldots,l_{2n}^{(0)})^T$, $L_{2n}^{(1)} = (l_0^{(1)}, l_1^{(1)},\ldots,l_{2n}^{(1)})^T$, $L_{2m}^{(2)} = (l_0^{(2)},l_1^{(2)},\ldots,l_{2m}^{(2)})^T$ and $L_{2m}^{(3)} = (l_0^{(3)},l_1^{(3)},\ldots,l_{2m}^{(3)})^T$ with

$$l_i = \begin{cases} C_n^{i/2}, & i = 0,2,4,\ldots,2n, \\ 0, & i = 1,3,5,\ldots,2n-1, \end{cases}$$

$$l_i^{(0)} = \begin{cases} C_{2n}^i & i = 0,2,4,\ldots,2n, \\ -C_{2n}^i, & i = 1,3,5,\ldots,2n-1, \end{cases}$$

$$l_i^{(1)} = \begin{cases} C_{n-2}^{i/2} - 2C_{n-2}^{i/2-1} + C_{n-2}^{i/2-2} - C_{2n}^i, & i = 0,2,4,\ldots,2n, \\ C_{2n}^i, & i = 1,3,5,\ldots,2n-1, \end{cases}$$

$$l_i^{(2)} = \begin{cases} 4C_{m-2}^{i/2-1}, & i = 0,2,4,\ldots,2m-2, \\ 0, & i = 1,3,5,\ldots,2m-1, \\ -2^m, & i = 2m. \end{cases}$$

$$l_i^{(3)} = \begin{cases} 0 & i = 0,1,2,\ldots,2m-1, \\ 2^m, & i = 2m, \end{cases}$$

Suppose that $n \geq m$, then we have

$$\left(1+x^2\right)^{n-m} \cdot \left[4x^2\left(1+x^2\right)^{m-2} - 2^m x^{2m}\right] = X_{2(n-m)}L_{2(n-m)} \cdot X_{2m}L_{2m}^{(2)} = X_{2n}\widetilde{L}_{2n}^{(2)},$$

$$\left(1+x^2\right)^{n-m} \cdot 2^m x^{2m} = X_{2(n-m)}L_{2(n-m)} \cdot X_{2m}L_{2m}^{(3)} = X_{2n}\widetilde{L}_{2n}^{(3)},$$

where $\widetilde{L}_{2n}^{(2)}=(\widetilde{l}_0^{(2)},\widetilde{l}_1^{(2)},\ldots,\widetilde{l}_{2n}^{(2)})^T$ and $\widetilde{L}_{2n}^{(3)}=(\widetilde{l}_0^{(3)},\widetilde{l}_1^{(3)},\ldots,\widetilde{l}_{2n}^{(3)})^T$ with

$$\widetilde{l}_k^{(2)}=\sum_{i+j=k} l_i l_j^{(2)},\quad i=0,1,\ldots,2(n-m),\ j=0,1,\ldots,2m,\ k=0,1,\ldots,2n,$$

$$\widetilde{l}_k^{(3)}=\sum_{i+j=k} l_i l_j^{(3)},\quad i=0,1,\ldots,2(n-m),\ j=0,1,\ldots,2m,\ k=0,1,\ldots,2n.$$

Therefore, by using the following transformation formula between the power basis and the classical Bernstein basis

$$X_{2n}=B_{2n}(x)M_{2n},$$

where $B_{2n}(x)=(b_{2n}^0(x),b_{2n}^1(x),\ldots,b_{2n}^{2n}(x))$, $b_{2n}^i(x)=C_{2n}^i(1-x)^{2n-i}x^i$, $i=0,1,\ldots,2n$, and

$$\{M_{2n}\}_{i,j}=\frac{C_i^j}{C_{2n}^j},\quad i,j=0,1,\ldots,2n,$$

we can immediately rewrite the four trigonometric Bernstein-like basis functions (2.16) into the following rational Bernstein form

$$(T_0(t;n),T_1(t;n),T_2(t;m),T_3(t;m))=\frac{B_{2n}(x)\left(M_{2n}L_{2n}^{(0)},M_{2n}L_{2n}^{(1)},M_{2n}\widetilde{L}_{2n}^{(2)},M_{2n}\widetilde{L}_{2n}^{(3)}\right)}{B_{2n}(x)M_{2n}L_{2n}}.$$

It follows that the TB-like curve $T(t;n,m)$ can be converted into the following rational Bézier curve of degree $2n$

$$T\,(t;n,m)=\frac{B_{2n}(x)\left(M_{2n}L_{2n}^{(0)},M_{2n}L_{2n}^{(1)},M_{2n}\widetilde{L}_{2n}^{(2)},M_{2n}\widetilde{L}_{2n}^{(3)}\right)}{B_{2n}(x)M_{2n}L_{2n}}(P_0,P_1,P_2,P_3)^T. \tag{2.17}$$

Similarly, for $m\ge n$, we can also convert the TB-like curve $T(t;n,m)$ into the following rational Bézier curve of degree $2m$

$$T\,(t;n,m)=\frac{B_{2m}(x)\left(M_{2m}\widetilde{L}_{2m}^{(0)},M_{2m}\widetilde{L}_{2m}^{(1)},M_{2m}L_{2m}^{(2)},M_{2m}L_{2m}^{(3)}\right)}{B_{2m}(x)M_{2m}L_{2m}}(P_0,P_1,P_2,P_3)^T, \tag{2.18}$$

where $\widetilde{L}_{2m}^{(0)}=(\widetilde{l}_0^{(0)},\widetilde{l}_1^{(0)},\ldots,\widetilde{l}_{2m}^{(0)})^T$ and $\widetilde{L}_{2m}^{(1)}=(\widetilde{l}_0^{(1)},\widetilde{l}_1^{(1)},\ldots,\widetilde{l}_{2m}^{(1)})^T$ with

$$\widetilde{l}_k^{(0)}=\sum_{i+j=k} l_i l_j^{(0)},\quad i=0,1,\ldots,2(m-n),\ j=0,1,\ldots,2n,\ k=0,1,\ldots,2m,$$

$$\widetilde{l}_k^{(1)}=\sum_{i+j=k} l_i l_j^{(1)},\quad i=0,1,\ldots,2(m-n),\ j=0,1,\ldots,2n,\ k=0,1,\ldots,2m.$$

From (2.17) and (2.18), we can see that a TB-like curve $T(t;n,m)$ can be converted into a special rational Bézier curve of degree $\max\{2n,2m\}$. Thus we can see that a quadratic TB-like curve $T(t;2,2)$ can be transformed to a special rational quartic Bézier curve. Fig. 2.7 gives some figure examples concerning the comparison between the TB-like curves and the rational cubic Bézier curves under the same control points. Although the trigonometric Bernstein-like basis has some properties analogous to that of the rational cubic Bernstein basis, for instance both the bases can represent exactly the elliptic and parabolic arcs, in the following discussion we shall see that the trigonometric Bernstein-like basis has some advantages on constructing spline curves with higher smoothness.

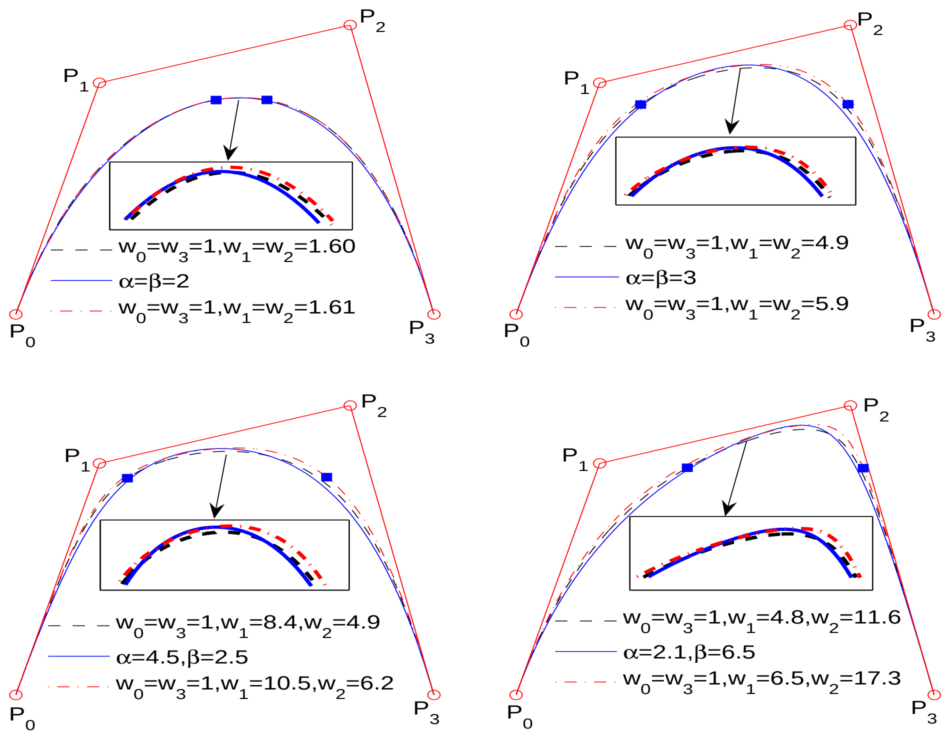


Fig. 2.7. TB-like curves and rational cubic Bézier curves.

## 3. Trigonometric B-spline-like Basis Functions

In this section, based on the trigonometric Bernstein-like basis functions given in (2.7), we shall construct a class of trigonometric B-spline-like basis functions with two local exponential shape parameters.

### 3.1. Construction of trigonometric B-spline-like basis functions

Given knots $u_0 < u_1 < \ldots < u_{n+4}$ and refer to $U = (u_0, u_1, \ldots, u_{n+4})$ as a knot vector. For $i = 0, 1, \ldots, n+3$, $\alpha_i, \beta_i \in [2, +\infty)$, let $h_i = u_{i+1} - u_i$ and $t_i(u) = \pi(u - u_i)/2h_i$, we want to construct a class of trigonometric B-spline-like basis functions as follows

$$B_i(u) = \begin{cases} d_i T_3\left(t_i; \beta_i\right), & u \in [u_i, u_{i+1}), \\ \sum_{j=0}^{3} c_{i+1,j} T_j\left(t_{i+1}; \alpha_{i+1}, \beta_{i+1}\right), & u \in [u_{i+1}, u_{i+2}), \\ \sum_{j=0}^{3} b_{i+2,j} T_j\left(t_{i+2}; \alpha_{i+2}, \beta_{i+2}\right), & u \in [u_{i+2}, u_{i+3}), \\ a_{i+3} T_0\left(t_{i+3}; \alpha_{i+3}\right), & u \in [u_{i+3}, u_{i+4}), \\ 0, & u \notin [u_i, u_{i+4}), \end{cases} \tag{3.1}$$

where $T_j(t_i;\alpha_i,\beta_i)$, $j = 0,1,2,3$ are the trigonometric Bernstein-like basis functions given in (2.7).

We want these trigonometric B-spline-like basis functions have $C^2$ continuity at each knot and form a partition of unity on the interval $[u_3, u_{n+1}]$. From these conditions, after some computation, we can deduce the coefficients $a_i, b_{i,j}, c_{i,j}, d_i$ as follows

$$\gamma_i = (\alpha_{i+1}-1)\,h_i + (\beta_i - 1)\,h_{i+1}, \qquad \lambda_i = \alpha_{i+1}h_i + \beta_i h_{i+1},$$

$$\phi_i = \frac{\alpha_{i+1}\gamma_i h_i}{2h_{i+1}^2} + \frac{\lambda_i}{\beta_i h_{i+1}}, \qquad \varphi_i = \frac{\beta_{i-1}\gamma_{i-1}h_i}{2h_{i-1}^2} + \frac{\lambda_{i-1}}{\alpha_i h_{i-1}},$$

$$a_i = \frac{2\alpha_{i-1}\beta_{i-2}\beta_{i-1}\gamma_{i-2}h_i^2}{\mu_{i-2}}, \qquad d_i = \frac{2\alpha_{i+1}\alpha_{i+2}\beta_{i+1}\gamma_{i+1}h_i^2}{\mu_i},$$

$$b_{i0} = \frac{\alpha_i h_{i-1}}{\lambda_{i-1}}\phi_i a_{i+1} + \frac{\beta_{i-1}h_i}{\lambda_{i-1}}\varphi_{i-1}d_{i-2},$$

$$c_{i0} = d_{i-1}, \quad b_{i1} = \phi_i a_{i+1}, \quad c_{i1} = \frac{\lambda_{i-1}}{\alpha_i h_{i-1}}d_{i-1},$$

$$b_{i2} = \frac{\lambda_i}{\beta_i h_{i+1}}a_{i+1}, \quad c_{i2} = \varphi_i d_{i-1}, \quad b_{i3} = a_{i+1},$$

$$c_{i3} = \frac{\alpha_{i+1}h_i}{\lambda_i}\phi_{i+1}a_{i+2} + \frac{\beta_i h_{i+1}}{\lambda_i}\varphi_i d_{i-1},$$

where $\mu_i = 2\alpha_{i+1}\beta_i\gamma_i\lambda_{i+1}h_{i+2} + \alpha_{i+1}\alpha_{i+2}\beta_i\beta_{i+1}\gamma_i\gamma_{i+1}h_{i+1} + 2\alpha_{i+2}\beta_{i+1}\gamma_{i+1}\lambda_i h_i$.

**Definition 3.1.** *Given a knot vector $U$, for any real numbers $\alpha_i, \beta_i \in [2, +\infty)$, with the coefficients $a_i, b_{i,j}, c_{i,j}, d_i$ given in the above expressions, the expressions* (3.1) *are defined to be the associated trigonometric B-spline-like basis functions.*

**Remark 3.1.** The trigonometric B-spline-like basis functions are constructed in the space

$$S := \{s \in C^2[u_0, u_{n+4}] \text{ s.t. } s\big|_{[u_i,u_{i+1}]} \in T_{\alpha_i,\beta_i}, \alpha_i, \beta_i \in [2,+\infty), i = 0,1,\ldots,n+3\},$$

where

$$T_{\alpha_i,\beta_i} := \text{span}\{1, \sin^2 t_i, (1-\sin t_i)^{\alpha_i}, (1-\cos t_i)^{\beta_i}\}.$$

In particular, for $u_{i+j} = u_i + jh, h > 0, j = 1,2,3,4$ and $\alpha_{i+1} = \alpha_{i+2} = \alpha_{i+3} = \beta_i = \beta_{i+1} = \beta_{i+2} = 3$, direct computation gives that

$$d_i = \frac{1}{10}, \quad c_{i+1,0} = \frac{1}{10}, \quad c_{i+1,1} = \frac{1}{5}, \quad c_{i+2,2} = \frac{4}{5}, \quad c_{i+3,3} = \frac{4}{5},$$

$$b_{i+2,0} = \frac{4}{5}, \quad b_{i+2,1} = \frac{4}{5}, \quad b_{i+2,2} = \frac{1}{5}, \quad b_{i+3,3} = \frac{1}{10}, \quad a_{i+3} = \frac{1}{10},$$

from which we can immediately obtain the following explicit expressions of $B_i(u)$

$$B_i(u)=\begin{cases}\frac{1}{10}(1-\cos t_i)^3, & u\in[u_i,u_i+h),\\ \frac{1}{10}(1-\sin t_{i+1})^3+\frac{1}{5}\sin t_{i+1}(1-\sin t_{i+1})(3-\sin t_{i+1}) & \\ +\frac{4}{5}\cos t_{i+1}(1-\cos t_{i+1})(3-\cos t_{i+1})+\frac{4}{5}(1-\cos t_{i+1})^3, & u\in[u_i+h,u_i+2h),\\ \frac{4}{5}(1-\sin t_{i+2})^3+\frac{4}{5}\sin t_{i+2}(1-\sin t_{i+2})(3-\sin t_{i+2}) & \\ +\frac{1}{5}\cos t_{i+2}(1-\cos t_{i+2})(3-\cos t_{i+2})+\frac{1}{10}(1-\cos t_{i+2})^3, & u\in[u_i+2h,u_i+3h),\\ \frac{1}{10}(1-\sin t_{i+3})^3, & u\in[u_i+3h,u_i+4h),\\ 0, & u\notin[u_i,u_i+4h).\end{cases}$$

For equidistant knots, we refer to the $B_i(u)$ as a uniform basis function and refer the knot vector $U$ as a uniform vector. For non-equidistant knots, $B_i(u)$ and $U$ are called a non-uniform basis function and a non-uniform knot vector, respectively. Fig. 3.1 shows some plots of trigonometric B-spline-like basis functions with different shape parameters. Before further discussion, we want to prove the following lemma, which is extremely useful for studying the partition of unity and the continuity of the trigonometric B-spline-like basis functions.

**Lemma 3.1.** *For all possible $i\in\mathbb{Z}^+$, $\alpha_i,\beta_i\in[2,+\infty)$, the coefficients $a_i,b_{i,j},c_{i,j},d_i$ have the following properties*

$$a_i+b_{i0}+c_{i0}=1,\quad b_{i1}+c_{i1}=1,\quad b_{i2}+c_{i2}=1,$$

$$b_{i3}+c_{i3}+d_i=1,\quad d_i=c_{i+1,0},\quad b_{i+2,0}=c_{i+1,3},\quad b_{i+2,3}=a_{i+3},$$

$$\left(\frac{\pi}{2h_i}\right)\beta_i d_i=\left(\frac{\pi}{2h_{i+1}}\right)\alpha_{i+1}\left(c_{i+1,1}-c_{i+1,0}\right),$$

$$\left(\frac{\pi}{2h_{i+1}}\right)\beta_{i+1}\left(c_{i+1,3}-c_{i+1,2}\right)=\left(\frac{\pi}{2h_{i+2}}\right)\alpha_{i+2}\left(b_{i+2,1}-b_{i+2,0}\right),$$

$$\left(\frac{\pi}{2h_{i+2}}\right)\beta_{i+2}\left(b_{i+2,3}-b_{i+2,2}\right)=-\left(\frac{\pi}{2h_{i+3}}\right)\alpha_{i+3}a_{i+3},$$

$$\left(\frac{\pi}{2h_i}\right)^2\left(\beta_i^2-\beta_i\right)d_i=\left(\frac{\pi}{2h_{i+1}}\right)^2\Big[\left(\alpha_{i+1}^2-\alpha_{i+1}\right)c_{i+1,0}-\left(2+\alpha_{i+1}^2-\alpha_{i+1}\right)c_{i+1,1}+2c_{i+1,2}\Big],$$

$$\left(\frac{\pi}{2h_{i+1}}\right)^2 \left[\left(\beta_{i+1}^2-\beta_{i+1}\right)c_{i+1,3}-\left(2+\beta_{i+1}^2-\beta_{i+1}\right)c_{i+1,2}+2c_{i+1,1}\right]$$

$$=\left(\frac{\pi}{2h_{i+2}}\right)^2 \left[\left(\alpha_{i+2}^2-\alpha_{i+2}\right)b_{i+2,0}-\left(2+\alpha_{i+2}^2-\alpha_{i+2}\right)b_{i+2,1}+2b_{i+2,2}\right],$$

$$\left(\frac{\pi}{h_{i+2}}\right)^2 \left[\left(\beta_{i+2}^2-\beta_{i+2}\right)b_{i+2,3}-\left(2+\beta_{i+2}^2-\beta_{i+2}\right)b_{i+2,2}+2b_{i+2,1}\right]$$

$$=\left(\frac{\pi}{h_{i+3}}\right)^2 \left(\alpha_{i+3}^2-\alpha_{i+3}\right)a_{i+3}.$$

*Proof.* From the expressions of the coefficients $a_i, b_{i,j}, c_{i,j}, d_i$ given above, it is obvious that $d_i = c_{i+1,0}$, $b_{i+2,0} = c_{i+1,3}$ and $b_{i+2,3} = a_{i+3}$. Straightforward computation gives that

$$\begin{aligned}
b_{i0} &= \frac{\alpha_i h_{i-1}}{\lambda_{i-1}}\phi_i a_{i+1} + \frac{\beta_{i-1}h_i}{\lambda_{i-1}}\varphi_{i-1}d_{i-2}\\
&= \frac{\alpha_i h_{i-1}}{\lambda_{i-1}}\left(1-\frac{2\alpha_{i+1}\beta_i\gamma_i\lambda_{i-1}h_{i-1}}{\mu_{i-1}}\right) + \frac{\beta_{i-1}h_i}{\lambda_{i-1}}\left(1-\frac{2\alpha_{i-1}\beta_{i-2}\gamma_{i-2}\lambda_{i-1}h_i}{\mu_{i-2}}\right)\\
&= 1 - a_i - d_{i-1}.
\end{aligned}$$

Similarly, $c_{i,3} = 1-a_{i+1}-d_i$. Thus we have $a_i+b_{i0}+c_{i0} = 1$ and $b_{i3}+c_{i3}+d_i = 1$. For $b_{i1}+c_{i1}$ and $b_{i2}+c_{i2}$, we have

$$\begin{aligned}
b_{i1}+c_{i1} &= \phi_i a_{i+1} + \frac{\lambda_{i-1}}{\alpha_i h_{i-1}}d_{i-1}\\
&= \left(\frac{\alpha_{i+1}\beta_i\gamma_i h_i + 2\lambda_i h_{i+1}}{2\beta_i h_{i+1}^2}\right)\frac{2\alpha_i\beta_{i-1}\beta_i\gamma_{i-1}h_{i+1}^2}{\mu_{i-1}} + \frac{\lambda_{i-1}}{\alpha_i h_{i-1}}\frac{2\alpha_i\alpha_{i+1}\beta_i\gamma_i h_{i-1}^2}{\mu_{i-1}}\\
&= \frac{\mu_{i-1}}{\mu_{i-1}} = 1,\\
b_{i2}+c_{i2} &= \frac{\lambda_i}{\beta_i h_{i+1}}a_{i+1} + \varphi_i d_{i-1}\\
&= \frac{\lambda_i}{\beta_i h_{i+1}}\frac{2\alpha_i\beta_{i-1}\beta_i\gamma_{i-1}h_{i+1}^2}{\mu_{i-1}} + \left(\frac{\alpha_i\beta_{i-1}\gamma_{i-1}h_i + 2\lambda_{i-1}h_{i-1}}{2\alpha_i h_{i-1}^2}\right)\frac{2\alpha_i\alpha_{i+1}\beta_i\gamma_i h_{i-1}^2}{\mu_{i-1}}\\
&= \frac{\mu_{i-1}}{\mu_{i-1}} = 1.
\end{aligned}$$

Direct computation gives that

$$\begin{aligned}
&\left(\frac{\pi}{2h_{i+1}}\right)\alpha_{i+1}\left(c_{i+1,1}-c_{i+1,0}\right)\\
=&\left(\frac{\pi}{2h_{i+1}}\right)\alpha_{i+1}\left(\frac{\lambda_i}{\alpha_{i+1}h_i}d_i - d_i\right) = \left(\frac{\pi}{2h_i}\right)\beta_i d_i,
\end{aligned}$$

$$
\begin{aligned}
&\left(\frac{\pi}{2h_{i+1}}\right)\beta_{i+1}\left(c_{i+1,3}-c_{i+1,2}\right)\\
=&\left(\frac{\pi}{2h_{i+1}}\right)\beta_{i+1}\left(\frac{\alpha_{i+2}h_{i+1}}{\lambda_{i+1}}\phi_{i+2}a_{i+3}+\frac{\beta_{i+1}h_{i+2}}{\lambda_{i+1}}\varphi_{i+1}d_i-\varphi_{i+1}d_i\right)\\
=&\left(\frac{\pi}{2h_{i+1}}\right)\beta_{i+1}\left(\frac{\alpha_{i+2}h_{i+1}}{\lambda_{i+1}}\phi_{i+2}a_{i+3}-\frac{\alpha_{i+2}h_{i+1}}{\lambda_{i+1}}\varphi_{i+1}d_i\right)\\
=&\left(\frac{\pi\alpha_{i+2}\beta_{i+1}}{2\lambda_{i+1}}\right)\left(\phi_{i+2}a_{i+3}-\varphi_{i+1}d_i\right),\\
&\left(\frac{\pi}{2h_{i+2}}\right)\alpha_{i+2}\left(b_{i+2,1}-b_{i+2,0}\right)\\
=&\left(\frac{\pi}{2h_{i+2}}\right)\alpha_{i+2}\left(\phi_{i+2}a_{i+3}-\frac{\alpha_{i+2}h_{i+1}}{\lambda_{i+1}}\phi_{i+2}a_{i+3}-\frac{\beta_{i+1}h_{i+2}}{\lambda_{i+1}}\varphi_{i+1}d_i\right)\\
=&\left(\frac{\pi}{2h_{i+2}}\right)\alpha_{i+2}\left(\frac{\beta_{i+1}h_{i+2}}{\lambda_{i+1}}\phi_{i+2}a_{i+3}-\frac{\beta_{i+1}h_{i+2}}{\lambda_{i+1}}\varphi_{i+1}d_i\right)\\
=&\left(\frac{\pi\alpha_{i+2}\beta_{i+1}}{2\lambda_{i+1}}\right)\left(\phi_{i+2}a_{i+3}-\varphi_{i+1}d_i\right),\\
&\left(\frac{\pi}{2h_{i+2}}\right)\beta_{i+2}\left(b_{i+2,3}-b_{i+2,2}\right)\\
=&\left(\frac{\pi}{2h_{i+2}}\right)\beta_{i+2}\left(a_{i+3}-\frac{\lambda_{i+2}}{\beta_{i+2}h_{i+3}}a_{i+3}\right)=-\left(\frac{\pi}{2h_{i+3}}\right)\alpha_{i+3}a_{i+3}.
\end{aligned}
$$

Furthermore, we have

$$
\begin{aligned}
&\left(\frac{\pi}{2h_{i+1}}\right)^2\left[\left(\alpha_{i+1}^2-\alpha_{i+1}\right)c_{i+1,0}-\left(2+\alpha_{i+1}^2-\alpha_{i+1}\right)c_{i+1,1}+2c_{i+1,2}\right]\\
=&\left(\frac{\pi}{2h_{i+1}}\right)^2\left[\left(\alpha_{i+1}^2-\alpha_{i+1}\right)\left(1-\frac{\lambda_i}{\alpha_{i+1}h_i}\right)+2\left(\varphi_{i+1}-\frac{\lambda_i}{\alpha_{i+1}h_i}\right)\right]d_i\\
=&\left(\frac{\pi}{2h_{i+1}}\right)^2\left[-\frac{\left(\alpha_{i+1}-1\right)\beta_ih_{i+1}}{h_i}+\frac{\beta_i\gamma_ih_{i+1}}{h_i^2}\right]d_i=\left(\frac{\pi}{2h_i}\right)^2\left(\beta_i^2-\beta_i\right)d_i,\\
&\left(\frac{\pi}{2h_{i+2}}\right)^2\left[\left(\beta_{i+2}^2-\beta_{i+2}\right)b_{i+2,3}-\left(2+\beta_{i+2}^2-\beta_{i+2}\right)b_{i+2,2}+2b_{i+2,1}\right]\\
=&\left(\frac{\pi}{2h_{i+2}}\right)^2\left[\left(\beta_{i+2}^2-\beta_{i+2}\right)\left(1-\frac{\lambda_{i+2}}{\beta_{i+2}h_{i+3}}\right)+2\left(\phi_{i+2}-\frac{\lambda_{i+2}}{\beta_{i+2}h_{i+3}}\right)\right]a_{i+3}\\
=&\left(\frac{\pi}{2h_{i+2}}\right)^2\left[-\frac{\alpha_{i+3}\left(\beta_{i+2}-1\right)h_{i+2}}{h_{i+3}}+\frac{\alpha_{i+3}\gamma_{i+2}h_{i+2}}{h_{i+3}^2}\right]a_{i+3}\\
=&\left(\frac{\pi}{2h_{i+3}}\right)^2\left(\alpha_{i+3}^2-\alpha_{i+3}\right)a_{i+3}.
\end{aligned}
$$

Finally, notice that $a_{i+3} = \left(\beta_{i+2}\mu_i h_{i+3}^2 d_i\right)/\left(\alpha_{i+1}\mu_{i+1}h_i^2\right)$, after some manipulations, we have

$$
\begin{aligned}
&\left(\frac{\pi}{2h_{i+1}}\right)^2 \left[\left(\beta_{i+1}^2-\beta_{i+1}\right)c_{i+1,3}-\left(2+\beta_{i+1}^2-\beta_{i+1}\right)c_{i+1,2}+2c_{i+1,1}\right]\\
=&\left(\frac{\pi}{2h_{i+1}}\right)^2 \Bigg[\left(\beta_{i+1}^2-\beta_{i+1}\right)\left(\frac{\alpha_{i+2}h_{i+1}}{\lambda_{i+1}}\phi_{i+2}a_{i+3}+\frac{\beta_{i+1}h_{i+2}}{\lambda_{i+1}}\varphi_{i+1}d_i-\varphi_{i+1}d_i\right)\\
&+2\left(\frac{\lambda_i}{\alpha_{i+1}h_i}-\varphi_{i+1}\right)d_i\Bigg]\\
=&\left(\frac{\pi}{2}\right)^2\frac{d_i}{\alpha_{i+1}\lambda_{i+1}\mu_{i+1}h_i^2h_{i+1}}\left[\alpha_{i+2}\beta_{i+1}\left(\beta_{i+1}-1\right)\beta_{i+2}\phi_{i+2}\mu_i h_{i+3}^2\right.\\
&\left.-\alpha_{i+1}\alpha_{i+2}\beta_{i+1}\left(\beta_{i+1}-1\right)\varphi_{i+1}\mu_{i+1}h_i^2-\alpha_{i+1}\beta_i\gamma_i\lambda_{i+1}\mu_{i+1}\right]\\
=&-\left(\frac{\pi}{2}\right)^2\frac{2\alpha_{i+2}\beta_{i+1}\gamma_{i+1}}{\mu_i\mu_{i+1}}\left\{\alpha_{i+1}\alpha_{i+2}\alpha_{i+3}\beta_i\beta_{i+1}\beta_{i+2}\left[\left(\beta_{i+1}-1\right)h_{i+1}+\left(\alpha_{i+2}-1\right)h_{i+2}\right]\right.\\
&+2\alpha_{i+1}\alpha_{i+3}\beta_i\beta_{i+2}\gamma_i\gamma_{i+2}\lambda_{i+1}+2\alpha_{i+2}\alpha_{i+3}\beta_{i+1}\left(\beta_{i+1}-1\right)\beta_{i+2}\gamma_{i+2}\lambda_i h_i\\
&\left.+2\alpha_{i+1}\alpha_{i+2}\left(\alpha_{i+2}-1\right)\beta_i\beta_{i+1}\gamma_i\lambda_{i+2}h_{i+3}\right\},
\end{aligned}
$$

$$
\begin{aligned}
&\left(\frac{\pi}{2h_{i+2}}\right)^2 \left[\left(\alpha_{i+2}^2-\alpha_{i+2}\right)b_{i+2,0}-\left(2+\alpha_{i+2}^2-\alpha_{i+2}\right)b_{i+2,1}+2b_{i+2,2}\right]\\
=&\left(\frac{\pi}{2h_{i+2}}\right)^2 \Bigg[\left(\alpha_{i+2}^2-\alpha_{i+2}\right)\left(\frac{\alpha_{i+2}h_{i+1}}{\lambda_{i+1}}\phi_{i+2}a_{i+3}+\frac{\beta_{i+1}h_{i+2}}{\lambda_{i+1}}\varphi_{i+1}d_i-\phi_{i+2}a_{i+3}\right)\\
&+2\left(\frac{\lambda_{i+2}}{\beta_{i+2}h_{i+3}}-\phi_{i+2}\right)a_{i+3}\Bigg]\\
=&\left(\frac{\pi}{2}\right)^2\frac{a_{i+3}}{\beta_{i+2}\lambda_{i+1}\mu_i h_{i+2}h_{i+3}^2}\left[\alpha_{i+1}\alpha_{i+2}\left(\alpha_{i+2}-1\right)\beta_{i+1}\varphi_{i+1}\mu_{i+1}h_i^2\right.\\
&\left.-\alpha_{i+2}\left(\alpha_{i+2}-1\right)\beta_{i+1}\beta_{i+2}\phi_{i+2}\mu_i h_{i+3}^2-\alpha_{i+3}\beta_{i+2}\gamma_{i+2}\lambda_{i+1}\mu_i\right]\\
=&-\left(\frac{\pi}{2}\right)^2\frac{2\alpha_{i+2}\beta_{i+1}\gamma_{i+1}}{\mu_i\mu_{i+1}}\left\{\alpha_{i+1}\alpha_{i+2}\alpha_{i+3}\beta_i\beta_{i+1}\beta_{i+2}\left[\left(\beta_{i+1}-1\right)h_{i+1}+\left(\alpha_{i+2}-1\right)h_{i+2}\right]\right.\\
&+2\alpha_{i+1}\alpha_{i+3}\beta_i\beta_{i+2}\gamma_i\gamma_{i+2}\lambda_{i+1}+2\alpha_{i+2}\alpha_{i+3}\beta_{i+1}\left(\beta_{i+1}-1\right)\beta_{i+2}\gamma_{i+2}\lambda_i h_i\\
&\left.+2\alpha_{i+1}\alpha_{i+2}\left(\alpha_{i+2}-1\right)\beta_i\beta_{i+1}\gamma_i\lambda_{i+2}h_{i+3}\right\}.
\end{aligned}
$$

These imply the lemma. □

### 3.2. Properties of the trigonometric B-spline-like basis functions

**Theorem 3.1.** *For all possible $i \in \mathbb{Z}^+$, $\alpha_i, \beta_i \in [2, +\infty)$, the set $\{B_0(u), B_1(u), \ldots, B_n(u)\}$ is linearly independent on $[u_3, u_{n+1}]$.*

*Proof.* For $\xi_i \in \mathbb{R}$ (i = 0, 1, ..., n), $u \in [u_3, u_{n+1}]$, let

$$S(u) = \sum_{i=0}^{n} \xi_i B_i(u) = 0.$$

For any $\alpha_i, \beta_i \in [2, +\infty)$, direct computation gives that

$$S(u_i) = a_i\xi_{i-3} + b_{i0}\xi_{i-2} + c_{i0}\xi_{i-1} = 0,$$

$$S'(u_i) = \frac{\pi}{2h_i}\left[\alpha_i a_i(\xi_{i-2} - \xi_{i-3}) + \frac{\beta_{i-1}d_{i-1}h_i}{h_{i-1}}(\xi_{i-1} - \xi_{i-2})\right] = 0,$$

$$S''(u_i) = \left(\frac{\pi}{2h_i}\right)^2\left[\alpha_i(\alpha_i - 1)a_i(\xi_{i-3} - \xi_{i-2}) + \frac{\beta_{i-1}(\beta_{i-1} - 1)d_{i-1}h_i^2}{h_{i-1}^2}(\xi_{i-1} - \xi_{i-2})\right] = 0,$$

where $i = 3, 4, \ldots, n+1$. Thus we can obtain linear systems with respect to $\xi_{i-3}$, $\xi_{i-2}$, $\xi_{i-1}$ as follows

$$\begin{cases} a_i\xi_{i-3} + b_{i0}\xi_{i-2} + c_{i0}\xi_{i-1} = 0, \\ \alpha_i a_i(\xi_{i-2} - \xi_{i-3}) + \frac{\beta_{i-1}d_{i-1}h_i}{h_{i-1}}(\xi_{i-1} - \xi_{i-2}) = 0, \\ \alpha_i(\alpha_i - 1)a_i(\xi_{i-3} - \xi_{i-2}) + \frac{\beta_{i-1}(\beta_{i-1}-1)d_{i-1}h_i^2}{h_{i-1}^2}(\xi_{i-1} - \xi_{i-2}) = 0. \end{cases}$$

Since $a_i + b_{i0} + c_{i0} = 1$, for the determinant of the coefficient matrix $D_i$ given by the above linear systems, by adding the first and the third column to the second column respectively, we have

$$\begin{aligned} |D_i| &= \begin{vmatrix} a_i & 1 & c_{i0} \\ -\alpha_i a_i & 0 & \frac{\beta_{i-1}d_{i-1}h_i}{h_{i-1}} \\ \alpha_i(\alpha_i - 1)a_i & 0 & \frac{\beta_{i-1}(\beta_{i-1}-1)d_{i-1}h_i^2}{h_{i-1}^2} \end{vmatrix} \\ &= \frac{\alpha_i\beta_{i-1}a_i d_{i-1}h_i}{h_{i-1}^2}\left[(\alpha_i - 1)h_{i-1} + (\beta_{i-1} - 1)h_i\right] > 0. \end{aligned}$$

Therefore, we can conclude that $\xi_{i-3} = \xi_{i-2} = \xi_{i-1} = 0$ for $i = 3, 4, \ldots, n+1$. These imply the theorem. □

**Theorem 3.2.** *The trigonometric B-spline-like basis functions* (3.1) *hold*

$$\sum_{i=0}^{n} B_i(u) = 1, \quad u \in [u_3, u_{n+1}].$$

*Proof.* For $u \in [u_i, u_{i+1}), i = 3, 4, \ldots, n$, since $B_j(u) = 0$ for $j \neq i-3, i-2, i-1, i$, and

$$B_{i-3}(u) = a_i T_0(t_i; \alpha_i), \quad B_{i-2}(u) = \sum_{j=0}^{3} b_{ij} T_j(t_i; \alpha_i, \beta_i),$$

$$B_{i-1}(u) = \sum_{j=0}^{3} c_{ij} T_j\left(t_i; \alpha_i, \beta_i\right), \quad B_i(u) = d_i T_3\left(t_i; \beta_i\right),$$

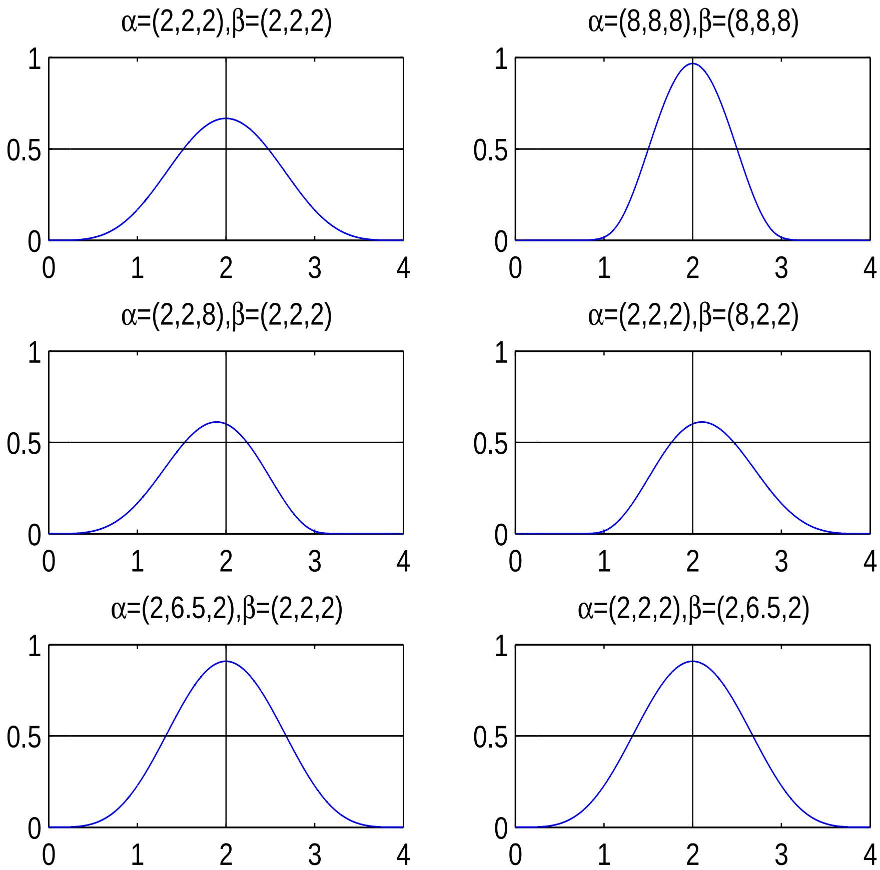


Fig. 3.1. Some plots of trigonometric B-spline-like basis functions with different shape parameters.

we have

$$\begin{aligned}\sum_{j=0}^{n} B_j(u) &= a_i T_0(t_i;\alpha_i) + \sum_{j=0}^{3} b_{ij} T_j(t_i;\alpha_i,\beta_i) + \sum_{j=0}^{3} c_{ij} T_j(t_i;\alpha_i,\beta_i) + d_i T_3(t_i;\beta_i)\\ &= \sum_{j=0}^{3} T_j(t_i;\alpha_i,\beta_i) = 1.\end{aligned}$$

These imply the theorem. □

**Theorem 3.3.** *For any* $\alpha_i, \beta_i \in [2, +\infty)$ *, the basis functions given in* (3.1) *hold* $B_i(u) > 0$*, for* $u_i < u < u_{i+4}$*.*

*Proof.* For all possible $\alpha_i, \beta_i \in [2, +\infty)$, it is obvious that the coefficients $a_i$, $b_{ij}$, $c_{ij}$ and $d_i$ are all positive numbers. Thus, from the nonnegativity of the trigonometric Bernstein-like basis functions $T_j(t_i;\alpha_i,\beta_i)$, $j = 0,1,2,3$, we can immediately conclude that $B_i(u) > 0$ for $u_i < u < u_{i+4}$. □

In view of Theorems 3.2 and 3.3, we say that the trigonometric B-spline-like basis functions (3.1) form a partition of unity and the function $B_i(u)$ has a support on the interval $[u_i, u_{i+4}]$.

**Theorem 3.4.** *For $u \in [u_i, u_{i+1}]$, $i = 3, 4, \ldots, n$, the system $(B_{i-3}(u), B_{i-2}(u), B_{i-1}(u), B_i(u))$ is a normalized totally positive basis of the space span $T_{\alpha_i,\beta_i}$.*

*Proof.* For $u \in [u_i, u_{i+1}]$, $t_i(u) = \pi (u - u_i)/2h_i$, $\alpha_i, \beta_i \in [2, +\infty)$, $i = 3, 4, \ldots, n$, it can be easily checked that

$$(B_{i-3}(u), B_{i-2}(u), B_{i-1}(u), B_i(u)) = (T_0(t_i; \alpha_i), T_1(t_i; \alpha_i), T_2(t_i; \beta_i), T_3(t_i; \beta_i))\, H_i,$$

where

$$H_i = \begin{bmatrix} a_i & b_{i,0} & c_{i,0} & 0 \\ 0 & b_{i,1} & c_{i,1} & 0 \\ 0 & b_{i,2} & c_{i,2} & 0 \\ 0 & b_{i,3} & c_{i,3} & d_i \end{bmatrix}.$$

From Theorem 2.2, since the system $(T_0(t_i; \alpha_i), T_1(t_i; \alpha_i), T_2(t_i; \beta_i), T_3(t_i; \beta_i))$ is the normalized optimal totally positive basis of the space $T_{\alpha_i,\beta_i}$, by Theorem 4.2 of [5], it is sufficient to conclude that $H_i$ is a nonsingular stochastic and totally positive matrix.

For any $\alpha_i, \beta_i \in [2, +\infty)$, it is obvious that $a_i$, $b_{i,j}$ $c_{i,j}$, $d_i > 0$, for all possible $i \in \mathbb{Z}^+$, $j = 0, 1, 2, 3$. In addition, from Lemma 1, we can see that $H_i$ is stochastic. In order to prove that $H_i$ is a totally positive matrix, we need to check that all its minors are nonnegative. By directly computing, we have

$$\begin{vmatrix} b_{i,0} & c_{i,0} \\ b_{i,1} & c_{i,1} \end{vmatrix} = \frac{\beta_{i-1}\varphi_{i-1}h_i}{\alpha_i h_{i-1}} d_{i-2}d_{i-1} > 0,$$

$$\begin{vmatrix} b_{i,0} & c_{i,0} \\ b_{i,2} & c_{i,2} \end{vmatrix} = \frac{1}{4\beta_i\lambda_{i-1}h_{i-1}h_{i+1}^2} \left[2\alpha_i\beta_{i-1}\gamma_{i-1}\lambda_i h_i h_{i+1} + \alpha_i\alpha_{i+1}\beta_{i-1}\beta_i\gamma_{i-1}\gamma_i h_i^2 \right.$$
$$\left. +2\alpha_{i+1}\beta_i\gamma_i\lambda_{i-1}h_{i-1}h_i\right] a_{i+1}d_{i-1} + \frac{\beta_{i-1}\varphi_{i-1}\varphi_i h_i}{\lambda_{i-1}} d_{i-2}d_{i-1} > 0,$$

$$\begin{vmatrix} b_{i,0} & c_{i,0} \\ b_{i,3} & c_{i,3} \end{vmatrix} = \frac{\alpha_i\alpha_{i+1}\phi_i\phi_{i+1}h_{i-1}h_i}{\lambda_{i-1}\lambda_i} a_{i+1}a_{i+2} + \frac{1}{4\lambda_{i-1}\lambda_i h_{i-1}h_{i+1}} \left[2\alpha_i\beta_{i-1}\gamma_{i-1}\lambda_i h_i h_{i+1} \right.$$
$$\left. + \alpha_i\alpha_{i+1}\beta_{i-1}\beta_i\gamma_{i-1}\gamma_i h_i^2 + 2\alpha_{i+1}\beta_i\gamma_i\lambda_{i-1}h_{i-1}h_i\right] a_{i+1}d_{i-1}$$
$$+ \frac{\alpha_{i+1}\beta_{i-1}\phi_{i+1}\varphi_{i-1}h_i^2}{\lambda_{i-1}\lambda_i} a_{i+2}d_{i-2} + \frac{\beta_{i-1}\beta_i\varphi_{i-1}\varphi_i h_i h_{i+1}}{\lambda_{i-1}\lambda_i} d_{i-2}d_{i-1} > 0,$$

$$\begin{vmatrix} b_{i,1} & c_{i,1} \\ b_{i,2} & c_{i,2} \end{vmatrix} = \frac{1}{4\alpha_i\beta_i h_{i-1}^2 h_{i+1}^2} \left[2\alpha_i\beta_{i-1}\gamma_{i-1}\lambda_i h_i h_{i+1} + \alpha_i\alpha_{i+1}\beta_{i-1}\beta_i\gamma_{i-1}\gamma_i h_i^2 \right.$$
$$\left. +2\alpha_{i+1}\beta_i\gamma_i\lambda_{i-1}h_{i-1}h_i\right] a_{i+1}d_{i-1} > 0,$$

$$\begin{vmatrix} b_{i,1} & c_{i,1} \\ b_{i,3} & c_{i,3} \end{vmatrix} = \frac{\alpha_{i+1}\phi_i\phi_{i+1}h_i}{\lambda_i} a_{i+1}a_{i+2} + \frac{1}{4\alpha_i\lambda_i h_{i-1}^2 h_{i+1}} \left[2\alpha_i\beta_{i-1}\gamma_{i-1}\lambda_i h_i h_{i+1} \right.$$

$$\left. + \alpha_i\alpha_{i+1}\beta_{i-1}\beta_i\gamma_{i-1}\gamma_i h_i^2 + 2\alpha_{i+1}\beta_i\gamma_i\lambda_{i-1}h_{i-1}h_i\right] a_{i+1}d_{i-1} > 0,$$

$$\begin{vmatrix} b_{i,2} & c_{i,2} \\ b_{i,3} & c_{i,3} \end{vmatrix} = \frac{\alpha_{i+1}\phi_{i+1}h_i}{\beta_i h_{i+1}} a_{i+1}a_{i+2} > 0.$$

From these, we can easily deduce that $H_i$ is nonsingular and all its remaining minors are nonnegative. These imply the theorem. □

**Theorem 3.5.** *With a non-uniform knot vector, the basis function $B_i(u)$ is $C^2$ continuous for $\alpha_i, \beta_i \in [2, +\infty)$ at each of the knots. With a uniform knot vector, the basis function $B_i(u)$ is $C^3$ continuous for $\alpha_{i+1} = \beta_i \in [2, +\infty)$ and $C^5$ continuous for all $\alpha_i = \beta_i = 3$ at each of the knots.*

*Proof.* Consider the continuity at the knot $u_{i+1}$. For any $\alpha_i, \beta_i \in [2, +\infty)$ we have

$$B_i(u_{i+1}^-) = d_i, \qquad B_i(u_{i+1}^+) = c_{i+1,0},$$

$$B_i'(u_{i+1}^-) = \left(\frac{\pi}{2h_i}\right)\beta_i d_i, \qquad B_i'(u_{i+1}^+) = \left(\frac{\pi}{2h_{i+1}}\right)\alpha_{i+1}\left(c_{i+1,1} - c_{i+1,0}\right),$$

$$B_i''(u_{i+1}^-) = \left(\frac{\pi}{2h_i}\right)^2 \left(\beta_i^2 - \beta_i\right) d_i,$$

$$B_i''(u_{i+1}^+) = \left(\frac{\pi}{2h_{i+1}}\right)^2 \left[\left(\alpha_{i+1}^2 - \alpha_{i+1}\right) c_{i+1,0} - \left(2 + \alpha_{i+1}^2 - \alpha_{i+1}\right) c_{i+1,1} + 2c_{i+1,2}\right],$$

$$B_i^{(3)}(u_{i+1}^-) = \left(\frac{\pi}{2h_i}\right)^3 \left(\beta_i^3 - 3\beta_i^2 + \beta_i\right) d_i,$$

$$B_i^{(3)}(u_{i+1}^+) = \left(\frac{\pi}{2h_{i+1}}\right)^3 \left(\alpha_{i+1}^3 - 3\alpha_{i+1}^2 + \alpha_{i+1}\right)\left(c_{i+1,1} - c_{i+1,0}\right).$$

From here and Lemma 3.1, for a non-uniform knot vector, we have $B_i(u_{i+1}^+) = B_i(u_{i+1}^-)$, $B_i'(u_{i+1}^+) = B_i'(u_{i+1}^-)$, $B_i''(u_{i+1}^+) = B_i''(u_{i+1}^-)$. In addition, for a uniform knot vector (that is all $h_i = h_{i+1}$) and $\alpha_{i+1} = \beta_i$, we have $d_i = c_{i+1,1} - c_{i+1,0}$, it follows that $B_i^{(3)}(u_{i+1}^+) = B_i^{(3)}(u_{i+1}^-)$.

Specially, for all $\alpha_i = \beta_i = 3$, direct computation gives that

$$B_i^{(4)}(u_{i+1}^-) = -8\left(\frac{\pi}{2h_i}\right)^4 (3d_i),$$

$$B_i^{(4)}(u_{i+1}^+) = -8\left(\frac{\pi}{2h_{i+1}}\right)^4 \left[3c_{i+1,0} - 4c_{i+1,1} + c_{i+1,2}\right],$$

$$B_i^{(5)}(u_{i+1}^-) = -57\left(\frac{\pi}{2h_i}\right)^5 d_i,$$

$$B_i^{(5)}(u_{i+1}^+) = -57\left(\frac{\pi}{2h_{i+1}}\right)^5 \left(c_{i+1,1} - c_{i+1,0}\right).$$

For a uniform knot vector and all $\alpha_i = \beta_i = 3$, we have $d_i = c_{i+1,1} - c_{i+1,0}$ and $3d_i = 3c_{i+1,0} - 4c_{i+1,1} + c_{i+1,2}$. These together we can immediately conclude that $B_i^{(4)}(u_{i+1}^+) = B_i^{(4)}(u_{i+1}^-)$

and $B_i^{(5)}(u_{i+1}^+) = B_i^{(5)}(u_{i+1}^-)$ for a uniform knot vector and all $\alpha_i = \beta_i = 3$. Thus the theorem follows at the knot $u_{i+1}$. We can deal with the continuity of the basis function $B_i(u)$ at other knots in the same way. □

### 3.3. Trigonometric B-spline-like curves

**Definition 3.2.** *Given a knot vector $U$ and control points $P_i$ $(i = 0, 1, \ldots, n)$ in $\mathbb{R}^2$ or $\mathbb{R}^3$, then, for $n \geq 3$, $u \in [u_3, u_{n+1}]$, $\alpha_i, \beta_i \in [2, +\infty)$,*

$$P(u) = \sum_{j=0}^{n} B_j(u) P_j, \tag{3.2}$$

*is called a trigonometric B-spline-like curve with two local exponential shape parameters $\alpha_i$ and $\beta_i$.*

Obviously, for $u \in [u_i, u_{i+1}]$, $3 \leq i \leq n$, the trigonometric B-spline-like curve $P(u)$ can be represented by the following curve segment

$$\begin{aligned} P(u) &= \sum_{j=i-3}^{i} B_j(u) P_j \\ &= (a_i P_{i-3} + b_{i0} P_{i-2} + c_{i0} P_{i-1})\, T_0(t_i; \alpha_i) + (b_{i1} P_{i-2} + c_{i1} P_{i-1})\, T_1(t_i; \alpha_i) \\ &\quad + (b_{i2} P_{i-2} + c_{i2} P_{i-1})\, T_2(t_i; \beta_i) + (b_{i3} P_{i-2} + c_{i3} P_{i-1} + d_i P_i)\, T_3(t_i; \beta_i), \end{aligned} \tag{3.3}$$

from which we can easily obtain the following end-point property of the curve

$$\begin{aligned}
&P(u_i^+) = a_i P_{i-3} + b_{i0} P_{i-2} + c_{i0} P_{i-1}, \\
&P(u_{i+1}^-) = b_{i3} P_{i-2} + c_{i3} P_{i-1} + d_i P_i, \\
&P'(u_i^+) = \left(\frac{\pi}{2h_i}\right) \left[\alpha_i a_i (P_{i-2} - P_{i-3}) + \frac{\beta_{i-1} d_{i-1} h_i}{h_{i-1}} (P_{i-1} - P_{i-2})\right], \\
&P'(u_{i+1}^-) = \left(\frac{\pi}{2h_i}\right) \left[\beta_i d_i (P_i - P_{i-1}) + \frac{\alpha_{i+1} a_{i+1} h_i}{h_{i+1}} (P_{i-1} - P_{i-2})\right], \\
&P''({u_i}^+) = \left(\frac{\pi}{2h_i}\right)^2 \left[\alpha_i(\alpha_i - 1) a_i (P_{i-3} - P_{i-2}) + \frac{\beta_{i-1}(\beta_{i-1} - 1) d_{i-1} h_i^2}{h_{i-1}^2} (P_{i-1} - P_{i-2})\right], \\
&P''(u_{i+1}^-) = \left(\frac{\pi}{2h_i}\right)^2 \left[\beta_i(\beta_i - 1) d_i (P_i - P_{i-1}) + \frac{\alpha_{i+1}(\alpha_{i+1} - 1) a_{i+1} h_i^2}{h_{i+1}^2} (P_{i-2} - P_{i-1})\right], \\
&P^{(3)}({u_i}^+) = \left(\frac{\pi}{2h_i}\right)^3 \left(\alpha_i^2 - 3\alpha_i + 1\right) \left[\alpha_i a_i (P_{i-2} - P_{i-3}) + \frac{\beta_{i-1} d_{i-1} h_i}{h_{i-1}} (P_{i-1} - P_{i-2})\right], \\
&P^{(3)}(u_{i+1}^-) = \left(\frac{\pi}{2h_i}\right)^3 \left(\beta_i^2 - 3\beta_i + 1\right) \left[\beta_i d_i (P_i - P_{i-1}) + \frac{\alpha_{i+1} a_{i+1} h_i}{h_{i+1}} (P_{i-1} - P_{i-2})\right].
\end{aligned}$$

Specially, for all $\alpha_i = \beta_i = 3$, we have

$$P^{(4)}(u_i^+) = -24\left(\frac{\pi}{2h_i}\right)^4 \left[a_i(P_{i-3} - P_{i-2}) + \frac{d_{i-1}h_i^2}{h_{i-1}^2}(P_{i-1} - P_{i-2})\right],$$

$$P^{(4)}(u_{i+1}^-) = -24\left(\frac{\pi}{2h_i}\right)^4 \left[d_i(P_i - P_{i-1}) + \frac{a_{i+1}h_i^2}{h_{i+1}^2}(P_{i-2} - P_{i-1})\right],$$

$$P^{(5)}(u_i^+) = -57\left(\frac{\pi}{2h_i}\right)^5 \left[a_i(P_{i-2} - P_{i-3}) + \frac{d_{i-1}h_i}{h_{i-1}}(P_{i-1} - P_{i-2})\right],$$

$$P^{(5)}(u_{i+1}^-) = -57\left(\frac{\pi}{2h_i}\right)^5 \left[d_i(P_i - P_{i-1}) + \frac{a_{i+1}h_i}{h_{i+1}}(P_{i-1} - P_{i-2})\right].$$

Based on Theorems 3.2 and 3.3, for $u \in [u_i, u_{i+1}]$, the trigonometric B-spline-like curve $P(u)$ lies in the convex hull of the points $P_{i-3}$, $P_{i-2}$, $P_{i-1}$ and $P_i$. Based on Theorem 3.4, the trigonometric B-spline-like curve $P(u)$ has variation diminishing property, which implies that the proposed new trigonometric B-spline-like curve $P(u)$ is suited for a good shape control.

Frenet continuity (FC) is often described in terms of the connection matrix, see [12, 28]. The trigonometric B-spline-like curve $P(u)$ is $FC^3$ at the knot $u_i$, if

$$\begin{bmatrix} P(u_i^+) \\ P'(u_i^+) \\ P''(u_i^+) \\ P'''(u_i^+) \end{bmatrix} = \begin{bmatrix} 1 & 0 & 0 & 0 \\ 0 & \omega_{11} & 0 & 0 \\ 0 & \omega_{21} & \omega_{11}^2 & 0 \\ 0 & \omega_{31} & \omega_{32} & \omega_{11}^3 \end{bmatrix} \begin{bmatrix} P(u_i^-) \\ P'(u_i^-) \\ P''(u_i^-) \\ P'''(u_i^-) \end{bmatrix}, \quad \omega_{11} > 0.$$

It was pointed out in [12] that $C^2 \cap FC^3$ is a reasonable smoothness property for application. From the end-point property of the trigonometric B-spline-like curve $P(u)$, we have the following result.

**Theorem 3.6.** *With a non-uniform knot vector, for any $\alpha_i, \beta_i \in [2, +\infty)$, the trigonometric B-spline-like curve $P(u)$ is $C^2 \cap FC^3$ continuous. With a uniform knot vector, $P(u)$ is $C^3$ continuous for all $\alpha_{i+1} = \beta_i \in [2, +\infty)$ and $C^5$ continuous for all $\alpha_i = \beta_i = 3$.*

*Proof.* Based on Theorem 3.5, we only need to prove that for any $\alpha_i, \beta_i \in [2, +\infty)$, the trigonometric B-spline-like curve $P(u)$ is $FC^3$ continuous for a non-uniform knot vector. In fact, from the end-point property of the curve $P(u)$, direct computation gives that

$$P_{i-1} - P_{i-2} = \frac{2\alpha_i(\alpha_i - 1)a_i h_i}{\pi\,|D_i|}P'(u_i) + \frac{4\alpha_i a_i h_i^2}{\pi^2\,|D_i|}P''(u_i),$$

$$P_{i-2} - P_{i-3} = \frac{2\beta_{i-1}(\beta_{i-1} - 1)d_{i-1}h_i^3}{\pi h_{i-1}^2\,|D_i|}P'(u_i) - \frac{4\beta_{i-1}d_{i-1}h_i^3}{\pi^2 h_{i-1}\,|D_i|}P''(u_i),$$

where $|D_i| = \alpha_i\beta_{i-1}a_i d_{i-1}h_i\left[(\alpha_i - 1)h_{i-1} + (\beta_{i-1} - 1)h_i\right]/h_{i-1}^2$. Thus, we are able to write the expression of $P^{(3)}(u_i{}^+) - P^{(3)}(u_i^-)$ as the following form

$$\begin{aligned} &P^{(3)}(u_i{}^+) - P^{(3)}(u_i^-) \\ =&\left(\frac{\pi}{2h_i}\right)^3 \left(\alpha_i^2 - 3\alpha_i + 1\right) \left[\alpha_i a_i (P_{i-2} - P_{i-3}) + \frac{\beta_{i-1} d_{i-1} h_i}{h_{i-1}} (P_{i-1} - P_{i-2})\right] \\ &- \left(\frac{\pi}{2h_{i-1}}\right)^3 \left(\beta_{i-1}^2 - 3\beta_{i-1} + 1\right) \left[\beta_{i-1} d_{i-1} (P_{i-1} - P_{i-2}) + \frac{\alpha_i a_i h_{i-1}}{h_i} (P_{i-2} - P_{i-3})\right] \\ &:= \omega_{31} P'(u_i) + \omega_{32} P''(u_i). \end{aligned}$$

These imply the theorem. □

Fig. 3.2 shows the space $C^2 \cap FC^3$ continuous and $C^2 \cap GC^3$ continuous curves with non-uniform knot vector and their corresponding torsion curves. The space $C^2 \cap FC^3$ continuous curves are generated by using the trigonometric B-spline-like basis with all $\alpha_i = \beta_i = 2$. And the space $C^2 \cap GC^3$ continuous curves are constructed by using the general quartic spline proposed in [23] with the choice of shape parameters $a_i = b_i = 0, c_i = 0.5$. The control points are $x_i = \cos(1.5i)/(1+0.15i), y_i = \sin(1.5i)/(1+0.15i), z_i = 1.5i, i = 0, 1, \ldots, 12$. The non-uniform knot vector is generated by using the Riesenfeld method described in [38]. In order to see more clearly the differences between the two space curves, we also give the porcupine plots of the normalized curvature along the main normal of the two generated space curves. From Fig. 3.2, it is observed that the space $C^2 \cap FC^3$ continuous are of more fairness than the $C^2 \cap GC^3$ continuous curves.

### 3.4. Local adjustable properties

The given spline curve $P(u)$ provides two local shape parameters $\alpha_i, \beta_i$. We can adjust the shape of the curve by changing the values of the shape parameters. From (3.3), we can know that shape parameters $\alpha_{i-1}$, $\alpha_i$, $\alpha_{i+1}$, $\alpha_{i+2}$, $\beta_{i-2}$, $\beta_{i-1}$, $\beta_i$, $\beta_{i+1}$ affect the curve segment $P(u)$, $u \in [u_i, u_{i+1}]$. Therefore, shape parameter $\alpha_i$ affects four curve segments $[u_{i-2}, u_{i+2}]$, and $\beta_i$ affects four curve segments $[u_{i-1}, u_{i+3}]$.

From (3.3), we can also predict the behavior of the curve $P(u)$. As $\alpha_i$ and $\beta_i$ increase, from (3.3) we can see that the coefficients of $P_{i-3}$ and $P_i$ decrease respectively, and the coefficients of $P_{i-2}$ and $P_{i-1}$ increase respectively. Moreover, as $\alpha_i$ and $\beta_i$ increase at the same time, then $P(u)$ tends to the edge $P_{i-2}P_{i-1}$. Thus the parameters $\alpha_i$ and $\beta_i$ serve to local control tension in the curve: increasing $\alpha_i$ and $\beta_i$ moves locally the curve segment $P(u)$ ($u \in [u_i, u_{i+1}]$) toward the edge $P_{i-2}P_{i-1}$ of the control polygon. And as $\alpha_i$ or $\beta_i$ increase respectively, $P(u)$ tends to the control point $P_{i-2}$ or $P_{i-1}$ respectively.

Fig. 3.3 shows open trigonometric B-spline-like curves with different shape parameters. On the left, the figure shows the trigonometric B-spline-like curves generated by setting all $\alpha_i = \beta_i = 2.1$ (solid lines), the dashed lines generated by changing one $\alpha_i$ to 4.2, and the dash-dotted lines generated by changing one $\beta_i$ to 5.5. The right figure shows the trigonometric B-spline-like curves generated by setting all $\alpha_i = \beta_i = 3$ for solid lines, $\alpha_i = \beta_i = 2$ for dashed lines, and $\alpha_i = \beta_i = 5$ for dash-dotted lines.

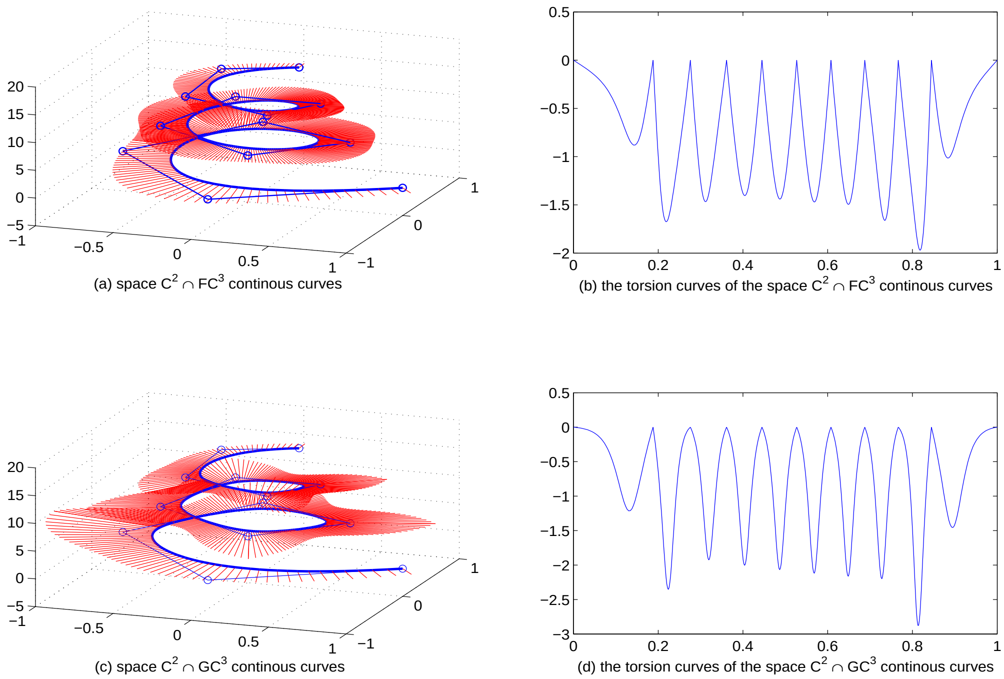


Fig. 3.2. Space $C^2 \cap FC^3$ continuous and $C^2 \cap GC^3$ continuous curves with non-uniform knot vector and their corresponding torsion curves.

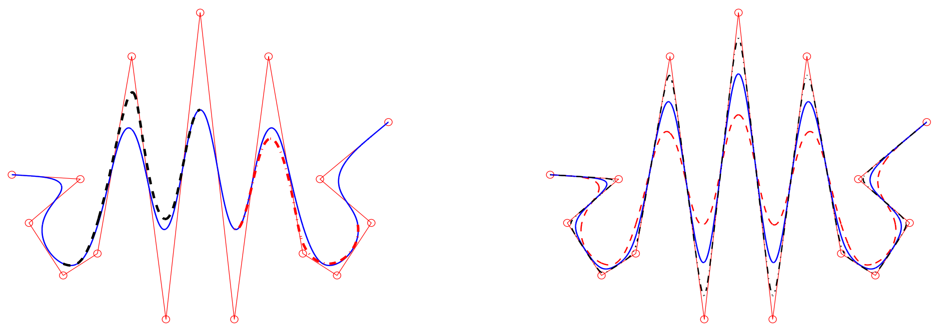

Fig. 3.3. Open trigonometric B-spline-like curves with uniform knot vector.

## 4. Trigonometric Bézier-like Basis Over Triangular Domain

Based on the trigonometric Bernstein-like basis given in (2.7), by using the method of tensor product, we can easily construct a class of trigonometric Bézier-like patch with four shape parameters over rectangular domain. Patch over triangular domain, however, is not a tensor product patch exactly. These imply that we cannot extend the trigonometric Bernstein-like basis (2.7) to the triangular domain by using the method of tensor product. In this section, we shall construct a new class of trigonometric Bézier-like basis over triangular domain with three shape parameters, which is a triangular domain extension of the trigonometric Bernstein-like basis given in (2.7).

### 4.1. Construction of the TB-like basis over triangular domain

**Definition 4.1.** *Let* $\alpha, \beta, \gamma \in [2, +\infty)$, *for* $D = \big\{(u, v, w)\,\big|\,u + v + w = \frac{\pi}{2}, u \geq 0, v \geq 0, w \geq 0\big\}$, *the following ten functions are defined as trigonometric Bézier-like (TB-like for short) basis functions, with three exponential shape parameters* $\alpha, \beta$ *and* $\gamma$, *over the triangular domain* $D$*:*

$$\begin{cases} T^3_{3,0,0}(u,v,w;\alpha,\beta,\gamma) = (1-\cos u)^{\alpha}, \\ T^3_{0,3,0}(u,v,w;\alpha,\beta,\gamma) = (1-\cos v)^{\beta}, \\ T^3_{0,0,3}(u,v,w;\alpha,\beta,\gamma) = (1-\cos w)^{\gamma}, \\ T^3_{2,1,0}(u,v,w;\alpha,\beta,\gamma) = \cos w \sin v (1-\cos u)\left[\dfrac{1+\cos u-(1-\cos u)^{\alpha-1}}{\cos u}\right], \\ T^3_{2,0,1}(u,v,w;\alpha,\beta,\gamma) = \cos v \sin w (1-\cos u)\left[\dfrac{1+\cos u-(1-\cos u)^{\alpha-1}}{\cos u}\right], \\ T^3_{1,2,0}(u,v,w;\alpha,\beta,\gamma) = \cos w \sin u (1-\cos v)\left[\dfrac{1+\cos v-(1-\cos v)^{\beta-1}}{\cos v}\right], \\ T^3_{0,2,1}(u,v,w;\alpha,\beta,\gamma) = \cos u \sin w (1-\cos v)\left[\dfrac{1+\cos v-(1-\cos v)^{\beta-1}}{\cos v}\right], \\ T^3_{1,0,2}(u,v,w;\alpha,\beta,\gamma) = \cos v \sin u (1-\cos w)\left[\dfrac{1+\cos w-(1-\cos w)^{\gamma-1}}{\cos w}\right], \\ T^3_{0,1,2}(u,v,w;\alpha,\beta,\gamma) = \cos u \sin v (1-\cos w)\left[\dfrac{1+\cos w-(1-\cos w)^{\gamma-1}}{\cos w}\right], \\ T^3_{1,1,1}(u,v,w;\alpha,\beta,\gamma) = 1 - \sum\limits_{\substack{i+j+k=3,\\ i\cdot j\cdot k\neq 1}} T^3_{i,j,k}(u,v,w;\alpha,\beta,\gamma). \end{cases} \tag{4.1}$$

**Remark 4.1.** Here, we give some hints on how to construct the TB-like basis over triangular domain (4.1). Our starting point is to extend the four univariate trigonometric Bernstein-like basis functions given in (2.7) to ten multi-variable basis functions over triangular domain such that the ten multi-variable basis functions can degenerate to the four univariate trigonometric Bernstein-like basis functions when one of the three variables is taken as zero and form a partition of unity. With these thoughts in mind, it is easy to construct the function $T^3_{3,0,0}(u,v,w;\alpha,\beta,\gamma)$ and symmetrically we can obtain the formulas of $T^3_{0,3,0}(u,v,w;\alpha,\beta,\gamma)$ and $T^3_{0,0,3}(u,v,w;\alpha,\beta,\gamma)$. Next, we shall construct the two functions $T^3_{2,1,0}(u,v,w;\alpha,\beta,\gamma)$ and $T^3_{2,0,1}(u,v,w;\alpha,\beta,\gamma)$ at the same time. Just like the circumstance of the classical Berstein-Bézier basis over triangular domain, when one of the three variables $w$ is taken as zero, the function $T^3_{2,1,0}(u,v,w;\alpha,\beta,\gamma)$ should degenerate to the univariate trigonometric Bernstein-like basis function $T_2(u;\alpha)$ (notice $v = \pi/2 - u$) and the function $T^3_{2,0,1}(u,v,w;\alpha,\beta,\gamma)$ should vanish. Analogously, when one of the three variables $v$ is taken as zero, we can get a similar conclusion that the function $T^3_{2,1,0}(u,v,w;\alpha,\beta,\gamma)$ should vanish while the function $T^3_{2,0,1}(u,v,w;\alpha,\beta,\gamma)$ should degenerate to the univariate trigonometric Bernstein-like basis function $T_2(u;\alpha)$. These give us a hint that the univariate trigonometric Bernstein-like basis function $T_2(u;\alpha)$ should be divided into two multi-variable functions and $T^3_{2,1,0}(u,v,w;\alpha,\beta,\gamma)$ is reasonable to possess the factor of $\cos w \sin v$ while $T^3_{2,0,1}(u,v,w;\alpha,\beta,\gamma)$ is reasonable to possess the factor of $\sin w \cos v$. From these and notice that $\cos u = \cos w \sin v + \sin w \cos v$ for $u+v+w=\pi/2$, we can immediately divide $T_2(u;\alpha)$ into a pair of multi-variable functions $T^3_{2,1,0}(u,v,w;\alpha,\beta,\gamma)$ and $T^3_{2,0,1}(u,v,w;\alpha,\beta,\gamma)$. By a similar way, we can obtain the other two pairs of multi-variable functions $T^3_{1,2,0}(u,v,w;\alpha,\beta,\gamma)$, $T^3_{0,2,1}(u,v,w;\alpha,\beta,\gamma)$ and $T^3_{1,0,2}(u,v,w;\alpha,\beta,\gamma)$, $T^3_{0,1,2}(u,v,w;\alpha,\beta,\gamma)$. And finally, considering the property of partition of unity, it is natural to obtain the formula of $T^3_{1,1,1}(u,v,w;\alpha,\beta,\gamma)$. Readers with an interest are also recommended to see [53], where a kind of polynomial Bernstein-Bézier-like basis over triangular domain with three exponential shape parameters can be found.

Obviously, when one of the three variables $w$ is taken as zero, the ten TB-like functions $T^3_{i,j,k}(u,v,w;\alpha,\beta,\gamma)$ degenerate to the trigonometric Bernstein-like basis functions $T_i(t;\alpha,\beta)$ (notice $v=\pi/2-u$) given in (2.7). Thus the TB-like functions $T^3_{i,j,k}(u,v,w;\alpha,\beta,\gamma)$ are the triangular domain extension of the the trigonometric Bernstein-like basis functions $T_i(t;\alpha,\beta)$.

**Remark 4.2.** For any $\alpha,\beta,\gamma \in [2,+\infty)$, we have

$$\lim_{u\to\pi/2}\left[\frac{1+\cos u-(1-\cos u)^{\alpha-1}}{\cos u}\right]=\lim_{u\to\pi/2}\left[\frac{-\sin u-(\alpha-1)\sin u(1-\cos u)^{\alpha-2}}{-\sin u}\right]=\alpha.$$

Similarly,

$$\lim_{v\to\pi/2}\left[\frac{1+\cos v-(1-\cos v)^{\beta-1}}{\cos v}\right]=\beta,\quad \lim_{w\to\pi/2}\left[\frac{1+\cos w-(1-\cos w)^{\gamma-1}}{\cos w}\right]=\gamma.$$

These imply that the definition of the TB-like basis functions over triangular domain given in (4.1) is meaningful.

Specially, for $m,n,l\in\mathbb{Z}^+$, $\alpha=1+m,\beta=1+n,\gamma=1+l$, we have

$$\begin{aligned}\frac{1+\cos u-(1-\cos u)^{\alpha-1}}{\cos u}&=1+\sum_{i=1}^{m}C_m^i(-\cos u)^{i-1},\\ \frac{1+\cos v-(1-\cos v)^{\beta-1}}{\cos v}&=1+\sum_{j=1}^{n}C_n^j(-\cos v)^{j-1},\\ \frac{1+\cos w-(1-\cos w)^{\gamma-1}}{\cos w}&=1+\sum_{k=1}^{l}C_l^k(-\cos w)^{k-1}.\end{aligned}$$

Fig. 4.1 shows some plots of TB-like basis functions over triangular domain. The three shape parameters take values $\alpha=\beta=\gamma=3.5$.

### 4.2. Properties of the TB-like basis over triangular domain

From the definition of the TB-like basis functions over triangular domain, we have the following important properties of the basis.

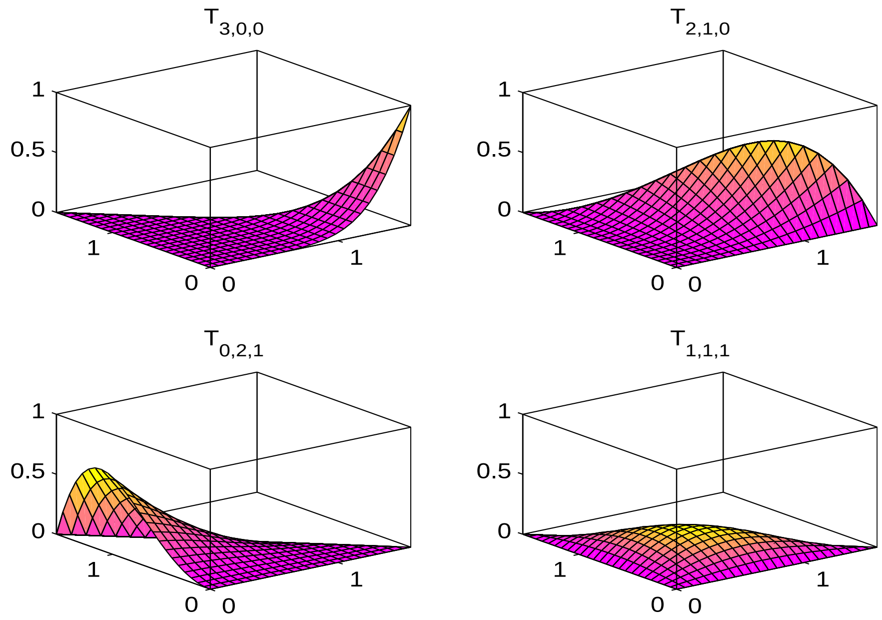


Fig. 4.1. Some plots of TB-like basis functions over triangular domain.

**Theorem 4.1.** *The TB-like basis functions over triangular domain given in* (4.1) *have the following properties:*

**(a)** *Nonnegativity.* $T^3_{i,j,k}(u,v,w;\alpha,\beta,\gamma) \geq 0, \quad i,j,k \in \mathbb{N}, i+j+k=3.$

**(b)** *Partition of unity.* $\sum\limits_{i+j+k=3} T^3_{i,j,k}(u,v,w;\alpha,\beta,\gamma) = 1.$

**(c)** *Linear independence. The set* $\left\{T^3_{i,j,k}(u,v,w;\beta,\alpha,\gamma); i,j,k \in \mathbb{N}, i+j+k=3\right\}$ *is linearly independent.*

**(d)** *Symmetry. For all* $i,j,k \in \mathbb{N}, i+j+k=3,$ *we have*

$$\begin{aligned}
&T^3_{i,j,k}(u,v,w;\alpha,\beta,\gamma) = T^3_{j,i,k}(v,u,w;\beta,\alpha,\gamma) = T^3_{j,k,i}(v,w,u;\beta,\gamma,\alpha)\\
&= T^3_{i,k,j}(u,w,v;\alpha,\gamma,\beta) = T^3_{k,i,j}(w,u,v;\gamma,\alpha,\beta) = T^3_{k,j,i}(w,v,u;\gamma,\beta,\alpha)
\end{aligned}$$

*Proof.* We shall prove $(a)$ and $(c)$. The remaining cases follow obviously.

**(a)** For any $\alpha,\beta,\gamma \geq 2, i,j,k \in \mathbb{N}, i+j+k=3$ and $i \cdot j \cdot k \neq 1$, it is obvious that $T^3_{i,j,k}(u,v,w;\alpha,\beta,\gamma) \geq 0$. Furthermore, for $T^3_{1,1,1}(u,v,w;\alpha,\beta,\gamma)$, since $u+v+w=\pi/2$, direct computation gives that

$$T^3_{1,1,1}(u,v,w;\alpha,\beta,\gamma) = 1 - \sum_{\substack{i+j+k=3,\\ i\cdot j\cdot k\neq 1}} T^3_{i,j,k}(u,v,w;\alpha,\beta,\gamma)$$

$$=1 - \left(\sin^2 u + \sin^2 v + \sin^2 w\right) = \frac{1}{2}\left(\cos 2u + \cos 2v + \cos 2w - 1\right)$$

$$=\cos(u+v)\cos(u-v) - \sin^2 w = \cos(u-v)\sin w - \cos(u+v)\sin w$$

$$=[\cos(u-v) - \cos(u+v)]\sin w = 2\sin u \sin v \sin w \geq 0.$$

**(c)** For any $\alpha,\beta,\gamma \in [2,+\infty)$, $\xi_{i,j,k} \in \mathbb{R}$ $(i,j,k \in \mathbb{N}, i+j+k=3)$, we consider a linear combination

$$\sum_{i+j+k=3} \xi_{i,j,k} T^3_{i,j,k}(u,v,w;\alpha,\beta,\gamma) = 0.$$

Let $w=0$, we have

$$\sum_{i=0}^{3} \xi_{i,3-i,0} T_i(u;\alpha,\beta) = 0. \tag{4.2}$$

Differentiate with respect to the variable $u$ on both sides, we have

$$\sum_{i=0}^{3} \xi_{i,3-i,0} T_i'(u;\alpha,\beta) = 0. \tag{4.3}$$

For $u=0$, from (4.2) and (4.3), we get linear system of equations with respect to $\xi_{0,3,0}$ and $\xi_{1,2,0}$ as follows

$$\xi_{0,3,0} = 0, \quad \beta\left(\xi_{1,2,0} - \xi_{0,3,0}\right) = 0.$$

Thus, we have $\xi_{0,3,0} = \xi_{1,2,0} = 0$. And for $u=\pi/2$, from (4.2) and (4.3), we have $\xi_{3,0,0} = \xi_{2,1,0} = 0$. Similarly, $\xi_{i,0,(3-i)} = \xi_{0,i,(3-i)} = 0$ for $i = 0,1,2,3$. And finally, $\xi_{1,1,1} = 0$. □

### 4.3. Triangular TB-like patch with three shape parameters

**Definition 4.2.** *Let $\alpha,\beta,\gamma \in [2,+\infty)$, given control points $P_{ij} \in \mathbb{R}^3$ $(i,j,k \in \mathbb{N}, i+j+k=3)$, and a domain triangle $D = \left\{(u,v,w)\,\middle|\, u+v+w = \frac{\pi}{2}, u\geq 0, v\geq 0, w\geq 0\right\}$, in which $(u,v,w)$ are the barycentric coordinates of the points in $D$. We call*

$$R(u,v,w) = \sum_{i+j+k=3} T^3_{i,j,k}(u,v,w;\alpha,\beta,\gamma) P_{i,j,k}, \quad (u,v,w)\in D, \tag{4.4}$$

*the trigonometric Bézier-like (TB-like for short) patch over triangular domain with three exponential shape parameters $\alpha,\beta,\gamma$.*

From the properties of the TB-like basis functions over triangular domain, some properties of the triangular TB-like patch, analogous to that of the triangular Bernstein-Bézier cubic patch, can be obtained as follows:

**(a)** affine invariance and convex hull property. Since the basis functions (4.1) have the properties of partition of unity and nonnegativity, these imply that the corresponding TB-like patch (4.4) has affine invariance and convex hull property.

**(b)** Geometric property at the corner points. Direct computation gives that

$$R(\pi/2, v, w) = P_{3,0,0}, R(u, \pi/2, w) = P_{0,3,0}, R(u, v, \pi/2) = P_{0,0,3}.$$

These indicate that the triangular TB-like patch interpolates at the corner points.

**(c)** Corner point tangent plane. Let $w = \pi/2 - u - v$, we have

$$\begin{aligned}
\left.\tfrac{\partial R(u,v,w)}{\partial u}\right|_{(\pi/2,0,0)} &= \alpha\left(P_{3,0,0} - P_{2,0,1}\right), & \left.\tfrac{\partial R(u,v,w)}{\partial v}\right|_{(\pi/2,0,0)} &= \alpha\left(P_{2,1,0} - P_{2,0,1}\right),\\
\left.\tfrac{\partial R(u,v,w)}{\partial u}\right|_{(0,\pi/2,0)} &= \beta\left(P_{1,2,0} - P_{0,2,1}\right), & \left.\tfrac{\partial R(u,v,w)}{\partial v}\right|_{(0,\pi/2,0)} &= \beta\left(P_{0,3,0} - P_{0,2,1}\right),\\
\left.\tfrac{\partial R(u,v,w)}{\partial u}\right|_{(0,0,\pi/2)} &= \gamma\left(P_{1,0,2} - P_{0,0,3}\right), & \left.\tfrac{\partial R(u,v,w)}{\partial v}\right|_{(0,0,\pi/2)} &= \gamma\left(P_{0,1,2} - P_{0,0,3}\right).
\end{aligned}$$

These indicate that the tangent plane at the three corner points $(\pi/2, 0, 0)$, $(0, \pi/2, 0)$, $(0, 0, \pi/2)$ are the three planes spanned by the control points $P_{3,0,0}$, $P_{2,1,0}$, $P_{2,0,1}$; $P_{0,3,0}$, $P_{1,2,0}$, $P_{0,2,1}$; $P_{0,0,3}$, $P_{1,0,2}$, $P_{0,1,2}$, respectively.

**(d)** Boundary property. For $w = 0$, $R(u, v, w)$ is just the following TB-like curve given in (2.9), with two shape parameters $\alpha$ and $\beta$

$$R(u, \pi/2 - u, 0) = \sum_{i=0}^{3} P_{i,3-i,0} T_i(u; \beta, \alpha). \tag{4.5}$$

Similarly, $R(0, v, \pi/2 - v)$ and $R(\pi/2 - w, 0, w)$ both are TB-like curves with shape parameters $\beta$, $\gamma$ and $\alpha$, $\gamma$, respectively. For $\alpha = \beta = 2$, the TB-like curve (2.9) can represent exactly elliptic and parabolic arcs, thus for $\alpha = \beta = \gamma = 2$, the three boundaries of triangular TB-like patch can be arcs of ellipse or parabola, respectively. Fig. 4.2 shows the triangular TB-like patch generated by setting $\alpha = \beta = \gamma = 2$. On the left, the figure shows the triangular TB-like patch whose boundaries are two elliptic arcs and a parabolic arc respectively. Its control points are $\{P_{3,0,0} = (0, -4, 0), P_{0,3,0} = (2, 0, 0), P_{0,0,3} = (0, 0, 1),$ $P_{2,1,0} = (1, -4, 0)$, $P_{2,0,1} = (0, -4, 1/2)$, $P_{1,2,0} = (2, 0, 0)$, $P_{0,2,1} = (2, 0, 1/2)$, $P_{1,0,2} = (0, -2, 1)$, $P_{0,1,2} = (1, 0, 1)$, $P_{1,1,1} = (1, -2, 1)\}$. The corresponding parametric equations of the three boundaries are: $u = 0$, $v = -4\sin x$, $w = \cos x$; $u = 2\sin x, v = 0, w = \cos x$; and $u = 2\cos x, v = -4 + 4\cos^2 x, w = 0$, where $x \in [0, \pi/2]$. On the right, the figure shows the triangular TB-like patch with three same boundaries as a quarter of the unit circle. The three boundaries are fitted onto the unit sphere. The associated control points of the triangular TB-like patch are $\{P_{3,0,0} = (0, 1, 0), P_{0,3,0} = (1, 0, 0), P_{0,0,3} = (0, 0, 1),$ $P_{2,1,0} = (1/2, 1, 0)$, $P_{2,0,1} = (0, 1, 1/2)$, $P_{1,2,0} = (1, 1/2, 0)$, $P_{0,2,1} = (1, 0, 1/2)$, $P_{1,0,2} = (0, 1/2, 1)$, $P_{0,1,2} = (1/2, 0, 1)$, $P_{1,1,1} = (1, -2, 1)\}$. The corresponding three parametric equations of the boundaries are: $u = 0, v = \sin x, w = \cos x$; $u = \sin x, v = 0, w = \cos x$; and $u = \cos x, v = \sin x, w = 0$, where $x \in [0, \pi/2]$.

**(e)** Shape adjustable property. Without changing the control net, we can adjust the shape of the triangular TB-like patch conveniently by using the three exponential shape parameters

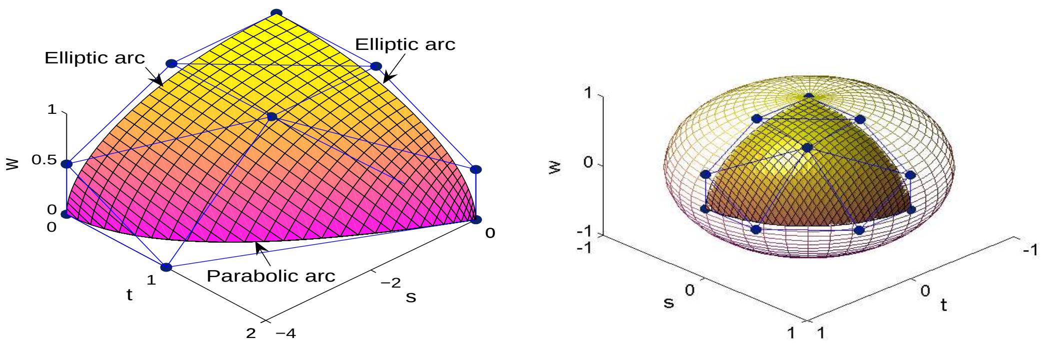


Fig. 4.2. Triangular TB-like patches whose boundaries are arcs of ellipse or parabola.

$\alpha, \beta$ and $\gamma$. As the three exponential shape parameters increase at the same time, the TB-like patch over triangular domain will be made close to the control net. Thus the three exponential shape parameters $\alpha, \beta, \gamma$ serve as tension parameters. In addition, from the boundary property of the triangular TB-like patch, we can see that the three shape parameters $\alpha$, $\beta$ and $\mu$ have nothing to do with the boundary curves $R(0, v, w)$, $R(u, 0, w)$ and $R(u, v, 0)$, respectively. It is equivalent to say that changing the values of single one shape parameter, one corresponding boundary curve will not change.

Fig. 4.3 shows the triangular TB-like patches and the effect on the patches by altering the values of the shape parameters under keeping the control net.

### 4.4. De Casteljau-type algorithm

The classical de Casteljau algorithm is a stable and efficient process for computing the triangular Bernstein-Bézier patch. Now we want to develop a de Casteljau-type algorithm for computing the proposed TB-like patch given in (4.4). For this goal, for any $(u, v, w) \in D$, let

$$f_1(u,v,w) := \frac{\sin u \cos w \left(\sin^2 u + \sin^2 v + \sin^2 w\right)}{\cos w \left(\sin u + \sin v\right) \left(\sin^2 u + \sin^2 v + \sin^2 w\right) + \sin w \left(\sin^2 u + \sin^2 v\right)},$$

$$f_2(u,v,w) := \frac{\sin v \cos w \left(\sin^2 u + \sin^2 v + \sin^2 w\right)}{\cos w \left(\sin u + \sin v\right) \left(\sin^2 u + \sin^2 v + \sin^2 w\right) + \sin w \left(\sin^2 u + \sin^2 v\right)},$$

$$f_3(u,v,w) := \frac{\sin w \left(\sin^2 u + \sin^2 v\right)}{\cos w \left(\sin u + \sin v\right) \left(\sin^2 u + \sin^2 v + \sin^2 w\right) + \sin w \left(\sin^2 u + \sin^2 v\right)},$$

$$g_1(u,v,w) := (1 - \cos u) \left(\sin^2 u + \sin^2 v + \sin^2 w\right),$$

$$g_2(u,v,w) := \sin v \cos w \left(\sin^2 u + \sin^2 v + \sin^2 w\right) + \sin u \sin v \sin w,$$

$$g_3(u,v,w) := \cos v \sin w \left(\sin^2 u + \sin^2 v + \sin^2 w\right) + \sin u \sin v \sin w,$$

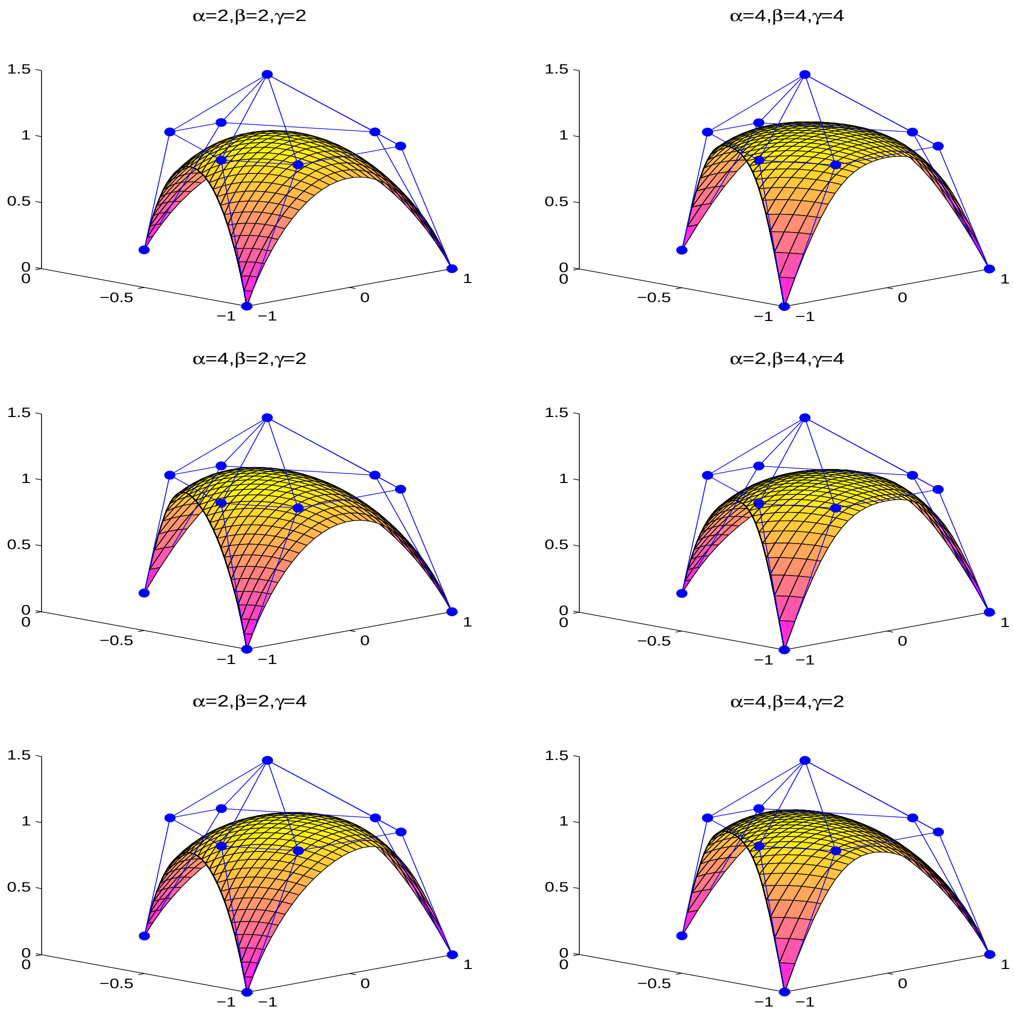


Fig. 4.3. Triangular TB-like patches with different shape parameters.

and

$$P^1_{2,0,0} := \frac{(1-\cos u)^{\alpha-2}}{1+\cos u}P_{3,0,0} + \frac{\left[1+\cos u-(1-\cos u)^{\alpha-2}\right]\sin v\cos w}{(1+\cos u)\cos u}P_{2,1,0} + \frac{\left[1+\cos u-(1-\cos u)^{\alpha-2}\right]\cos v\sin w}{(1+\cos u)\cos u}P_{2,0,1},$$

$$P^1_{0,2,0} := \frac{\left[1+\cos v-(1-\cos v)^{\beta-2}\right]\sin u\cos w}{(1+\cos v)\cos v}P_{1,2,0} + \frac{(1-\cos v)^{\beta-2}}{1+\cos v}P_{0,3,0} + \frac{\left[1+\cos v-(1-\cos v)^{\beta-2}\right]\cos u\sin w}{(1+\cos v)\cos v}P_{0,2,1},$$

$$P^1_{0,0,2} := \frac{\left[1+\cos w-(1-\cos w)^{\gamma-2}\right]\sin u\cos v}{(1+\cos w)\cos w}P_{1,0,2} + \frac{\left[1+\cos w-(1-\cos w)^{\gamma-2}\right]\cos u\sin v}{(1+\cos w)\cos w}P_{0,1,2} + \frac{(1-\cos w)^{\gamma-2}}{1+\cos w}P_{0,0,3},$$

$$P^1_{1,1,0} := f_1(u,v,w)P_{2,1,0} + f_2(u,v,w)P_{1,2,0} + f_3(u,v,w)P_{1,1,1},$$
$$P^1_{1,0,1} := f_1(u,w,v)P_{2,0,1} + f_3(u,w,v)P_{1,1,1} + f_2(u,w,v)P_{1,0,2},$$
$$P^1_{0,1,1} := f_3(v,w,u)P_{1,1,1} + f_1(v,w,u)P_{0,2,1} + f_2(v,w,u)P_{0,1,2}.$$

Then we can rewrite the expression of the TB-like patch (4.4) as follows

$$\begin{aligned} R(u,v,w) = {} & \frac{1-\cos^2 u}{\sin^2 u + \sin^2 v + \sin^2 w}\left[g_1(u,v,w)P^1_{2,0,0} + g_2(u,v,w)P^1_{1,1,0} + g_3(u,v,w)P^1_{1,0,1}\right] \\ & + \frac{1-\cos^2 v}{\sin^2 u + \sin^2 v + \sin^2 w}\left[g_2(v,u,w)P^1_{1,1,0} + g_1(v,u,w)P^1_{0,2,0} + g_3(v,u,w)P^1_{0,1,1}\right] \\ & + \frac{1-\cos^2 w}{\sin^2 u + \sin^2 v + \sin^2 w}\left[g_3(w,v,u)P^1_{1,0,1} + g_2(w,v,u)P^1_{0,1,1} + g_1(w,v,u)P^1_{0,0,2}\right]. \end{aligned} \tag{4.6}$$

Furthermore, by setting

$$P^2_{1,0,0} := g_1(u,v,w)P^1_{2,0,0} + g_2(u,v,w)P^1_{1,1,0} + g_3(u,v,w)P^1_{1,0,1},$$
$$P^2_{0,1,0} := g_2(v,u,w)P^1_{1,1,0} + g_1(v,u,w)P^1_{0,2,0} + g_3(v,u,w)P^1_{0,1,1},$$
$$P^2_{0,0,1} := g_3(w,v,u)P^1_{1,0,1} + g_2(w,v,u)P^1_{0,1,1} + g_1(w,v,u)P^1_{0,0,2},$$

we have

$$\begin{aligned} R(u,v,w) = {} & \frac{1-\cos^2 u}{\sin^2 u + \sin^2 v + \sin^2 w}P^2_{1,0,0} + \frac{1-\cos^2 v}{\sin^2 u + \sin^2 v + \sin^2 w}P^2_{0,1,0} \\ & + \frac{1-\cos^2 w}{\sin^2 u + \sin^2 v + \sin^2 w}P^2_{0,0,1} := P^3_{0,0,0}. \end{aligned} \tag{4.7}$$

For $u+v+w=\pi/2$, it is easy to check that $f_1(u,v,w)+f_2(u,v,w)+f_3(u,v,w)=1$and $g_1(u,v,w)+g_2(u,v,w)+g_3(u,v,w)=1$ (by using $\sin^2 u+\sin^2 v+\sin^2 w+2\sin u\sin v\sin w=1$). Thus (4.6) and (4.7) really describe a de Casteljau-type algorithm for computing the proposed TB-like patch (4.4).

### 4.5. Composite triangular TB-like patches

Let two triangular TB-like patches be

$$R_1(u,v,w) = \sum_{i+j+k=3} T^3_{i,j,k}(u,v,w;\alpha_1,\beta,\gamma)P_{i,j,k}, \quad (u,v,w)\in D, \tag{4.8}$$
$$R_2(u,v,w) = \sum_{i+j+k=3} T^3_{i,j,k}(u,v,w;\alpha_2,\beta,\gamma)Q_{i,j,k}, \quad (u,v,w)\in D, \tag{4.9}$$

respectively. It is apparent that if the control points satisfy

$$P_{0,j,k} = Q_{0,j,k}, \quad j,k\in\mathbb{N}, j+k=3, \tag{4.10}$$

the two patches join along common boundary curve: $R_1(0,v,w) = R_2(0,v,w), v+w=\pi/2$. Thus the two patches clearly form a surface with positional continuity, or a surface with $C^0$ continuity.

For the common boundary curve $R_1(0, v, \pi/2 - v)$, differentiate with respect to $v$, we have

$$\frac{dR_1(0, v, \pi/2 - v)}{dv} = \beta \sin v(1 - \cos v)^{\beta-1}(P_{0,3,0} - P_{0,2,1})$$
$$+ 2 \sin v \cos v(P_{0,2,1} - P_{0,1,2}) + \gamma \cos v(1 - \sin v)^{\gamma-1}(P_{0,1,2} - P_{0,0,3}). \quad (4.11)$$

For $R_1(u, v, \pi/2 - u - v)$ and $R_2(u, v, \pi/2 - u - v)$, differentiate with respect to $u$ respectively, we have

$$\left.\frac{\partial R_1(u, v, \pi/2 - u - v)}{\partial u}\right|_{u=0} = \beta \sin v(1 - \cos v)^{\beta-1}(P_{1,2,0} - P_{0,2,1})$$
$$+ 2 \sin v \cos v(P_{1,1,1} - P_{0,1,2}) + \gamma \cos v(1 - \sin v)^{\gamma-1}(P_{1,0,2} - P_{0,0,3}), \quad (4.12)$$
$$\left.\frac{\partial R_2(u, v, \pi/2 - u - v)}{\partial u}\right|_{u=0} = \beta \sin v(1 - \cos v)^{\beta-1}(Q_{1,2,0} - Q_{0,2,1})$$
$$+ 2 \sin v \cos v(Q_{1,1,1} - Q_{0,1,2}) + \gamma \cos v(1 - \sin v)^{\gamma-1}(Q_{1,0,2} - Q_{0,0,3}). \quad (4.13)$$

The condition for smooth joining is that the vectors defined by equations (4.11) through (4.13) be coplanar for any value of $v$, which can be expressed as

$$\left.\frac{\partial R_2(u, v, \pi/2 - u - v)}{\partial u}\right|_{u=0} = \phi \frac{dR_1(0, v, \pi/2 - v)}{dv} + \varphi \left.\frac{\partial R_1(u, v, \pi/2 - u - v)}{\partial u}\right|_{u=0},$$

where $\phi, \varphi$ both are constants. From these, we can immediately obtain the following rule

$$\begin{cases} Q_{1,2,0} - Q_{0,2,1} = \phi(P_{0,3,0} - P_{0,2,1}) + \varphi(P_{1,2,0} - P_{0,2,1}), \\ Q_{1,1,1} - Q_{0,1,2} = \phi(P_{0,2,1} - P_{0,1,2}) + \varphi(P_{1,1,1} - P_{0,1,2}), \\ Q_{1,0,2} - Q_{0,0,3} = \phi(P_{0,1,2} - P_{0,0,3}) + \varphi(P_{1,0,2} - P_{0,0,3}). \end{cases} \quad (4.14)$$

Summarizing the above discussion, we can conclude the following theorem.

**Theorem 4.2.** *For $\alpha_i, \beta, \gamma \in [2, +\infty), i = 1, 2$, the resulting surface composed by* (4.8) *and* (**??**) *is $G^1$ continuous, if the conditions* (4.10) *and* (4.14) *hold.*

From Theorem 4.2, we can see that the conditions for smooth joining two triangular TB-like patches are similar to those for joining two triangular Bernstein-Bézier cubic patches, see [41]. However, the shape of the obtained $G^1$ continuous surface can be modified conveniently by changing the exponential shape parameters in the triangular TB-like patches.

Fig. 4.4 shows the $G^1$ continuous composite triangular TB-like patches with different shape parameters. The parameters take values $\phi = 1, \varphi = -1$.

## 5. Conclusion

The four new proposed trigonometric Berntein-like basis functions possessing two exponential shape parameters form a normalized optimal totally positive basis and are useful for constructing curves in CAGD. The spectral analysis of the trigonometric Bernstein-like operator shows that the trigonometric Bézier-like curves are closer to the given control polygon than the cubic Bézier curves. The trigonometric B-spline-like basis has totally positive property and can be $C^2 \cap FC^3$ continuous for a non-uniform knot vector, and $C^3$ even $C^5$ continuous

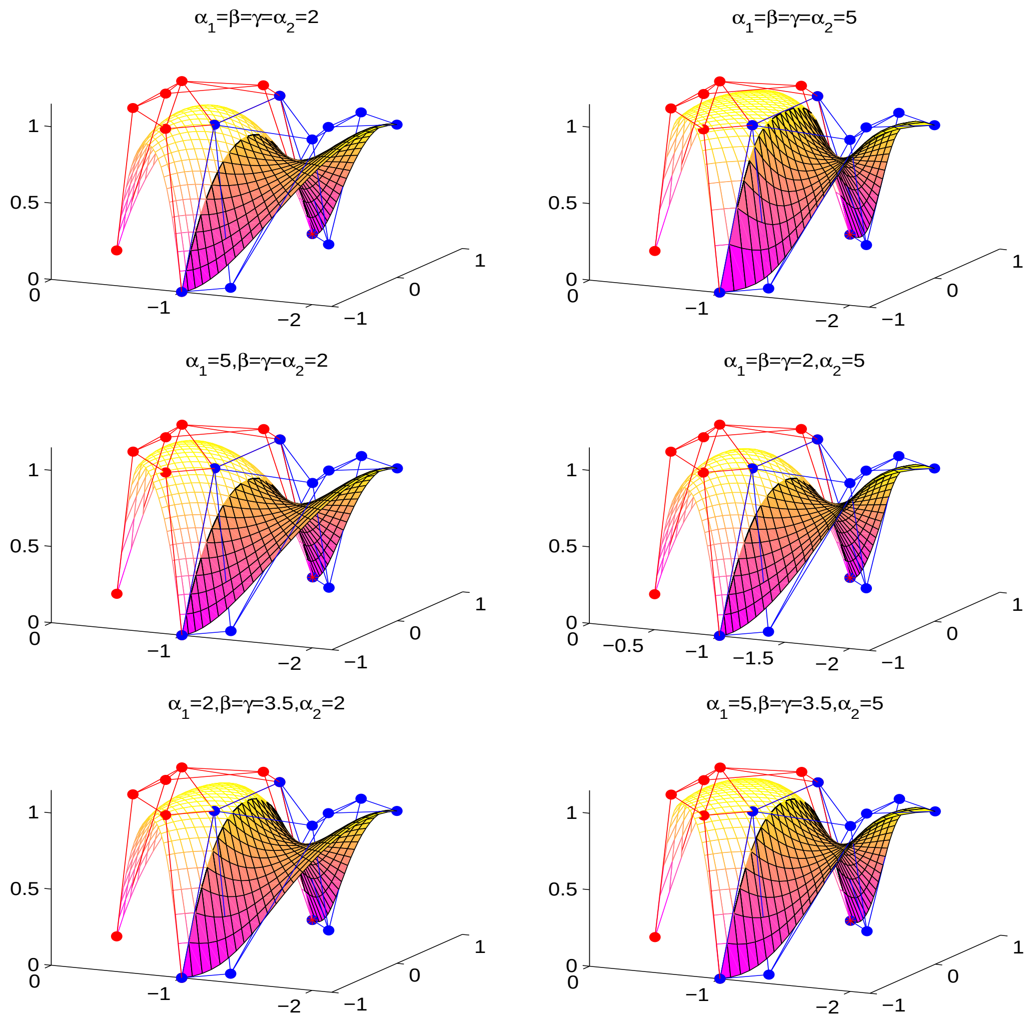


Fig. 4.4. $G^1$ continuous composite triangular TB-like patches.

for a uniform knot vector. Thus compared with the classical $C^2$ cubic non-uniform rational B-spline basis, the proposed trigonometric B-spline-like basis is suited for constructing space curves where the continuous torsion is required. With the exponential shape parameters, the corresponding trigonometric B-spline-like curves can move locally or globally toward the control polygon. The given trigonometric Bézier-like basis over triangular domain is a new construction for geometric design and computing, which is useful for constructing some surfaces whose boundaries are arcs of ellipse or parabola. There are also some work worthy of further study, such as subdivide algorithm and knot insertion technique for the new given spline curves. And $C^2 \cap FC^3$ continuity together with controllable tension property also means that the proposed trigonometric B-spline-like basis can be applied to construct shape preserving interpolating space curves. These will be our future work.

**Acknowledgments.** We wish to express our gratitude to the referees for their valuable remarks for improvements. The research is supported by the National Natural Science Foundation of China (No. 60970097, No. 11271376), Postdoctoral Science Foundation of China (2015M571931), and Graduate Students Scientific Research Innovation Project of Hunan Province (No. CX2012B111).

## References


[1] J.M. Aldaz, O. Kounchev and H. Render, Shape preserving properties of generalized Bernstein operators on Extended Chebyshev spaces, *Numer. Math.*, **114** (2009), 1–25.

[2] T. Bosner and M. Rogina, Numerically stable algorithem for cycloidal splines, *Ann. Univ. Ferrara*, **53** (2007), 189–197.

[3] T. Bosner and M. Rogina, Variable degree polynomial splines are Chebyshev splines, *Adv. Comput. Math.*, **38** (2013), 383–400.

[4] J.M. Carnicer and J.M. Peña, Shape preserving representations and optimality of the Bernstein basis, *Adv. Comput. Math.* **1** (1993), 173–196.

[5] J.M. Carnicer and J.M. Peña, Total positive bases for shape preserving curve design and optimality of B-splines, *Comput. Aided Geome. Des.*, **11** (1994), 635–656.

[6] J.M. Carnicer, E. Mainar and J.M. Peña, Critical length for design purposes and Extended Chebyshev Spaces, *Contr. Approx.*, **20** (2004), 55–71.

[7] J.M. Carnicer, E. Mainar and J.M. Peña, A Bernstein-like operator for a mixed algebraic–trigonometric space, *XXI Congreso de Ecuaciones Diferenciales y Aplicaciones*, *XI Congreso de Matemática Aplicada*, (2009), 1–7.

[8] J. Cao and G.Z. Wang, An extension of Bernstein-Bézier surface over the triangular domain, *Prog. Nat. Sci.*, **17** (2007), 352–357.

[9] S. Cooper and S. Waldron, The eigenstructure of the Bernstein operator, *J. Approx. Theory*, **105** (2000), 133–165.

[10] P. Costantini, Curve and surface construction using variable degree polynomial splines, *Comput. Aided Geome. Des.*, **17** (2000), 419–466.

[11] P. Costantini and F. Pelosi, Shape preserving approximation by space curves, *Numer. Alg.*, **27** (2001), 219–316.

[12] P. Costantini and C. Manni, Geometric construction of spline curves with tension properties, *Comput. Aided Geome. Des.*, **20** (2003), 579–599.

[13] P. Costantini and C. Manni, Shape-preserving $C^3$ interpolation: the curve case, *Adv. Comput. Math.*, **18** (2003), 41–63.

[14] P. Costantini and F. Pelosi, Shape preserving approximation of spatial data, *Adv. Comput. Math.* **20** (2004), 25–51.

[15] P. Costantini, T. Lyche and C. Manni, On a class of weak Tchebysheff systems, *Numer. Math.*, **101** (2005), 333–354.

[16] P. Costantini and F. Pelosi, Data approximation using shape preserving parametric surface, *SIAM J. Numer. Anal.*, **47** (2008), 20–47.

[17] W.W. Gao and Z.M. Wu, A quasi-interpolation scheme for periodic data based on multiquadric trigonometric B-splines, *J. Comput. Appl. Math.*, **271** (2014), 20–30.

[18] X.L. Han, Quadratic trigonometric polynomial curves with a shape parameter, *Comput. Aided Geome. Des.*, **19** (2002), 503–512.

[19] X.L. Han, Piecewise quadratic trigonometric polynomial curves, *Math. Comput.*, **243** (2003), 1369–1377.

[20] X.L. Han, Cubic trigonometric polynomial curves with a shape parameter, *Comput. Aided Geome. Des.*, **21** (2004), 535–548.

[21] X.L. Han, $C^2$ quadratic trigonometric polynomial curves with local bias, *J. Comput. Appl. Math.*, **180** (2005), 161–172.

[22] X.L. Han, Quadratic trigonometric polynomial curves concerning local control, *Appl. Numer. Math.*, **56** (2006), 105–115.

[23] X.L. Han, A class of general quartic spline curves with shape parameters, *Comput. Aided Geome. Des.*, **28** (2011), 151–163.

[24] X.L. Han and Y.P. Zhu, Curve construction based on five trigonometric blending functions, *BIT Numer. Math.*, **52** (2012), 953–979.

[25] X.A. Han, Y.C. Ma and X.L. Huang, The cubic trigonometric Bézier curve with two shape parameters, *Appl. Math. Lett.* **22** (2009), 226–231.

[26] M. Hoffmann, Y.J. Li and G.Z. Wang, Paths of C-Bézier curves, *Comput. Aided Geome. Des.*, **23** (2006), 463–475.

[27] M. Hoffmann, I. Juhász and G. Károlyi, A control point based curve with two exponential shape parameters, *BIT Numer. Math.*, **54** (2014), 691–710.

[28] J. Hoschek and D. Lasser, Fundamentals of Computer Aided Geometric Design. AK Peters, Wellesley, 1993.

[29] P.E. Koch, T. Lyche, M. Neamtu and L.L. Shumaker, Control curves and knot insertion for trigonometric splines, *Adv. Comput. Math.*, **3** (1995), 405–424.

[30] T. Lyche and T. Winther, A stable recurrence ralation for trigonometric polynomial curves, *J. Approx. Theory*, **25** (1979), 266–279.

[31] M.L. Mazure, Quasi-Chebychev splines with connexion matrices: application to variable degree polynomial splines, *Comput. Aided Geome. Des.*, **18** (2001), 287–298.

[32] M.L. Mazure, Blossoms and optimal bases, *Adv. Comput. Math.*, **20** (2004), 177–203.

[33] M.L. Mazure, On dimension elevation in quasi extended Chebyshev spaces, *Numer. Math.*, **109** (2008), 459–475.

[34] M.L. Mazure, Which spaces for design, *Numer. Math.*, **110** (2008), 357–392.

[35] M.L. Mazure, On a general new class of quasi Chebyshevian splines, *Numer. Alg.*, **58** (2011), 399–438.

[36] M.L. Mazure, Quasi Extended Chebyshev spaces and weight functions, *Numer. Math.*, **118** (2011), 79–108.

[37] C. Manni, F. Pelosi and M.L. Sampoli, Generalized B-splines as a tool in isogeometric analysis, *Comput. Methods Appl. Mech. Engrg.*, **200** (2011), 867–881.

[38] R.F. Riesenfeld, Non-uniform B-spline curves. In: Proceedings of Second USA-JAPAN Computer Conference, AFIPS, (1975), 551–555.

[39] J. Sánchez-Reyes, Harmonic rational Bézier curves, p-Bézier curves and trigonometric polynomials, *Comput. Aided Geome. Des.*, **15** (1998), 909-923.

[40] L.L. Schumaker, Spline Functions: Basic Theory, 3rd ed., Cambridge University Press, Cambridge, 2007.

[41] D. Salomon and F.B. Schneider, The Computer Graphics Manual. Springer, New York, 2011.

[42] W.Q. Shen and G.Z. Wang, Changeable degree spline basis functions, *J. Comput. Appl. Math.*, **234** (2010), 2516–2529.

[43] W.Q. Shen and G.Z. Wang, Triangular domain extension of linear Bernstein-like trigonometric polynomial basis, *J. Zhejiang Univ-Sci C (Comput & Electron)*, **11** (2010), 356–364.

[44] W.Q. Shen, G.Z. Wang and P. Yin, Explicit representations of changeable degree spline basis functions, *J. Comput. Appl. Math.*, **238** (2013), 39–50.

[45] G. Walz, Some identities for trigonometric B-splines with application to curve design, *BIT Numer. Math.*, **37** (1997), 189–201.

[46] G. Walz, Trigonometric Bézier and Stancu polynomials over intervals and triangles, *Comput. Aided Geome. Des.*, **14** (1997), 393–397.

[47] Z.M. Wu, Piecewise functions generated by the solutions of linear ordinary differential equations, *Stud. Adv. Math.*, **42** (2008), 769–784.

[48] Y.W. Wei, W.Q. Shen and G.Z. Wang, Triangular domain extension of algebraic trigonometric

Bézier-like basis, *Appl. Math. J. Chinese Univ.*, **26** (2011), 151–160.

[49] L.Q. Yang and X.M. Zeng, Bézier curves and surfaces with shape parameters, *Int. J. Comput. Math.* **86** (2009), 1253–1263.

[50] L.L. Yan and J.F. Liang, A class of algebraic-trigonometric blended splines, *J. Comput. Appl. Math.*, **235** (2011), 1713–1729.

[51] L.L. Yan and J.F. Liang, An extension of the Bézier model, *Appl. Math. Comput.*, **218** (2011), 2863–2879.

[52] J.W. Zhang, C-curves, an extension of cubic curves, *Comput. Aided Geome. Des.*, **13** (1996), 199–217.

[53] Y.P. Zhu and X.L. Han, A class of $\alpha\beta\gamma$-Bernstein-Bézier basis functions over triangular domain, *Appl. Math. Comput.*, **220** (2013), 446–454.

[54] Y.P. Zhu, X.L. Han and S.J. Liu, Curves construction based on four $\alpha\beta$-Bernstein-like basis functions, *J. Comput. Appl. Math.*, **273** (2015), 160–181.